Laboratoř růstových regulátorů

Miroslav Strnad

AUXINY
[kap. 19]

- Univerzita Palackého & Ústav experimentální botaniky AV CR

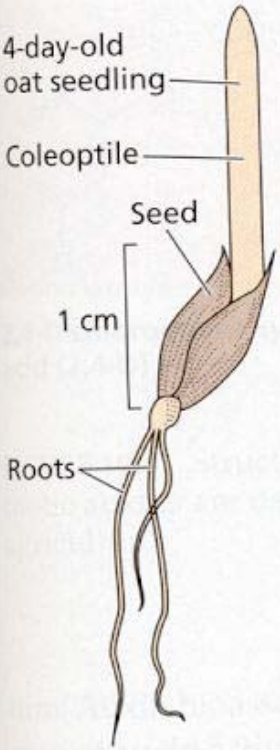

Darwin (1880)

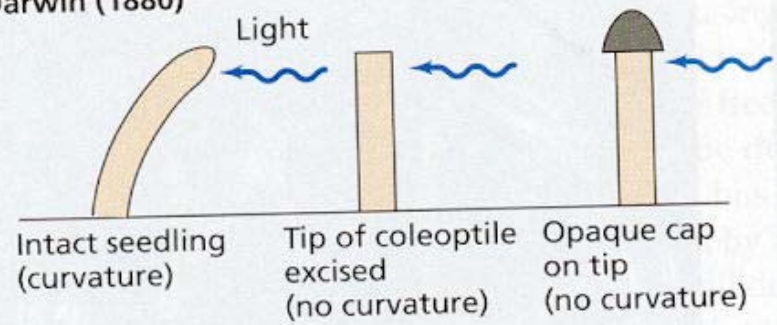

From experiments on coleoptile phototropism, Darwin concluded in 1880 that a growth stimulus is produced in the coleoptile tip and is transmitted to the growth zone.

Boysen-Jensen (1913)

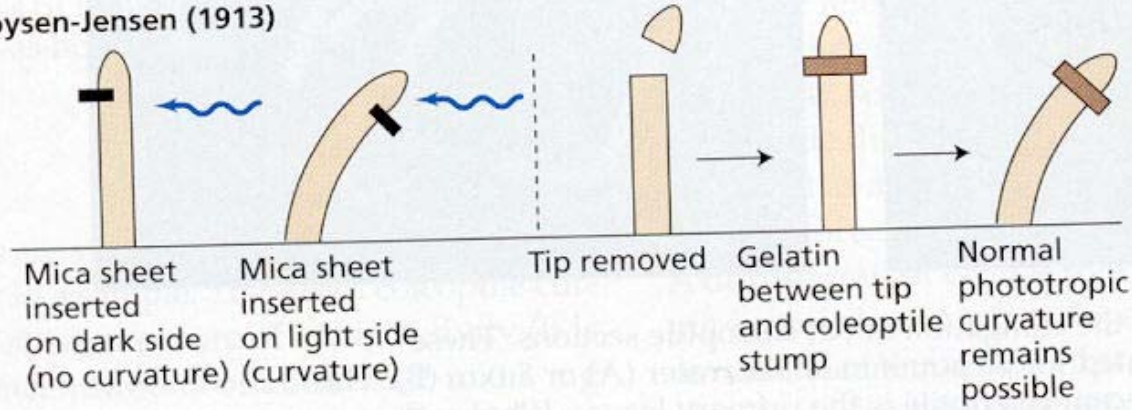

In 1913, P. Boysen-Jensen discovered that the growth stimulus passes through gelatin but not through water-impermeable barriers such as mica.

Paál (1919)

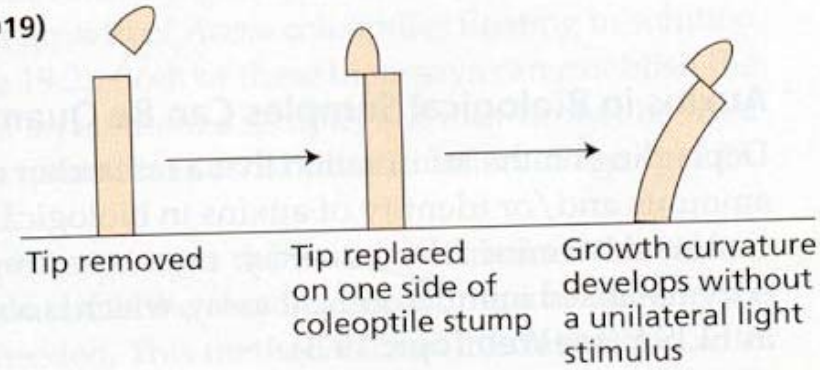

In 1919, A. Paál provided evidence that the growth-promoting stimulus produced in the tip was chemical in nature.

Went (1926)

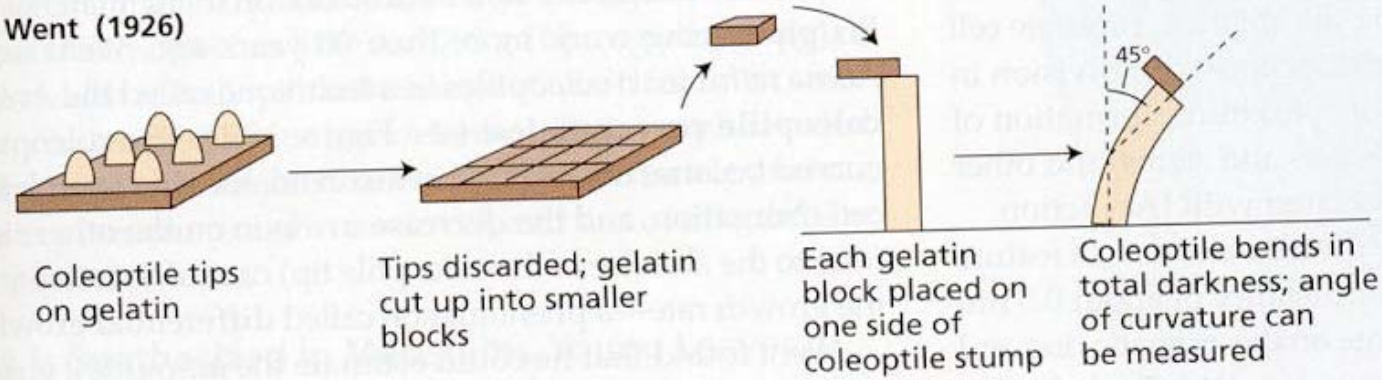

In 1926, F. W. Went showed that the active growth-promoting substance can diffuse into a gelatin block. He also devised a coleoptile-bending assay for quantitative auxin analysis.

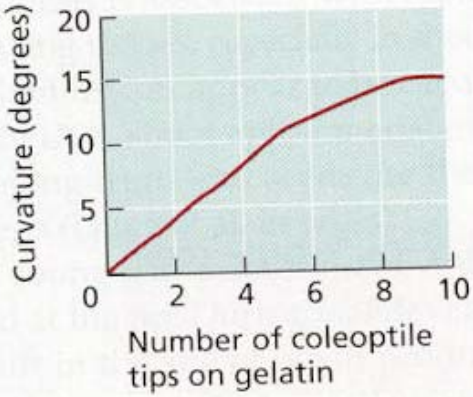

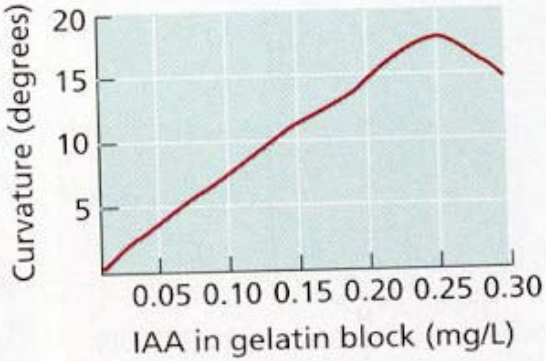

FIGURE 19.1 Summary of early experiments in auxin research.

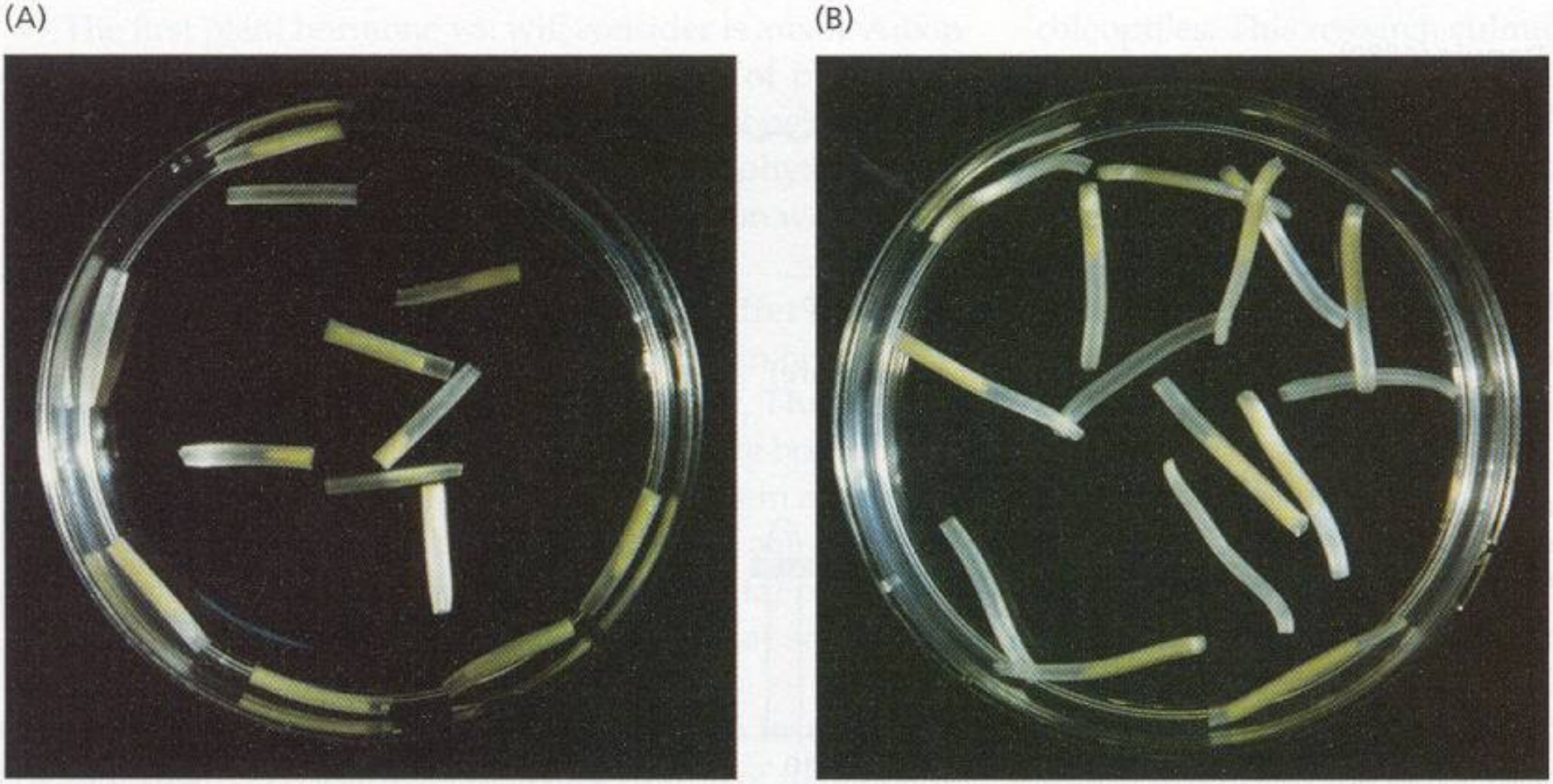

FIGURE 19.2 Auxin stimulates the elongation of oat coleoptile sections. These coleoptile sections were incubated for 18 hours in either water (A) or auxin (B). The yellow tissue inside the translucent coleoptile is the primary leaves. (Photos © M. B. Wilkins.)

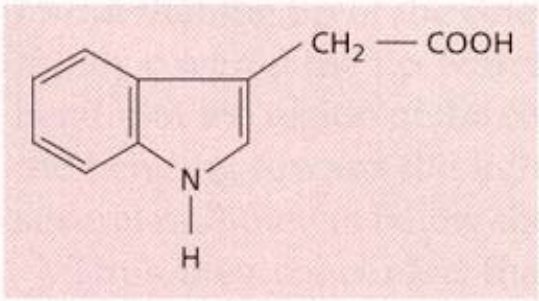

Indole-3-acetic acid
(IAA)

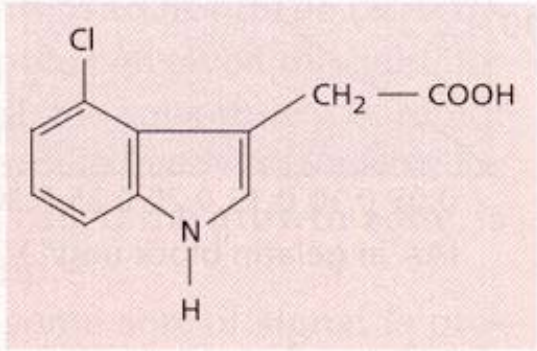

4-Chloroindole-3-acetic acid
(4-Cl-IAA)

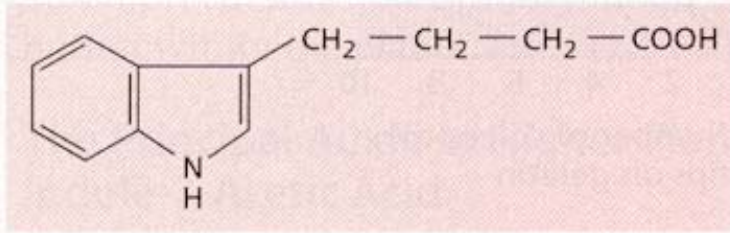

Indole-3-butyric acid
(IBA)

FIGURE 19.3 Structure of three natural auxins. Indole-3-acetic acid (IAA) occurs in all plants, but other related compounds in plants have auxin activity. Peas, for example, contain 4-chloroindole-3-acetic acid. Mustards and corn contain indole-3-butyric acid (IBA).

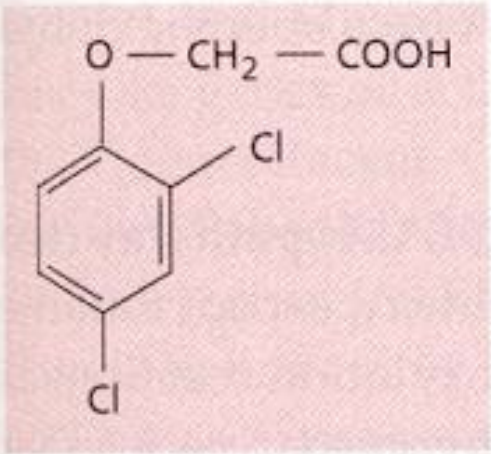

2,4-Dichlorophenoxyacetic acid (2,4-D)

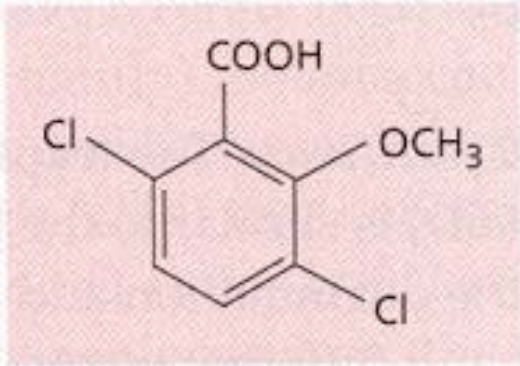

2-Methoxy-3, 6-dichlorobenzoic acid (dicamba)

FIGURE 19.4 Structures of two synthetic auxins. Most synthetic auxins are used as herbicides in horticulture and agriculture.

FIGURE 19.5 Detection of sites of auxin synthesis and transport in a young leaf primordium of *DR5 Arabidopsis* by means of a *GUS* reporter gene with an auxin-sensitive promoter. During the early stages of hydathode differentiation, a center of auxin synthesis is evident as a concentrated dark blue *GUS* stain (arrow) in the lobes of the serrated leaf margin. A gradient of diluted GUS activity extends from the margin toward a differentiating vascular strand (arrowhead), which functions as a sink for the auxin flow originating in the lobe. (Courtesy of R. Aloni and C. I. Ullrich.)

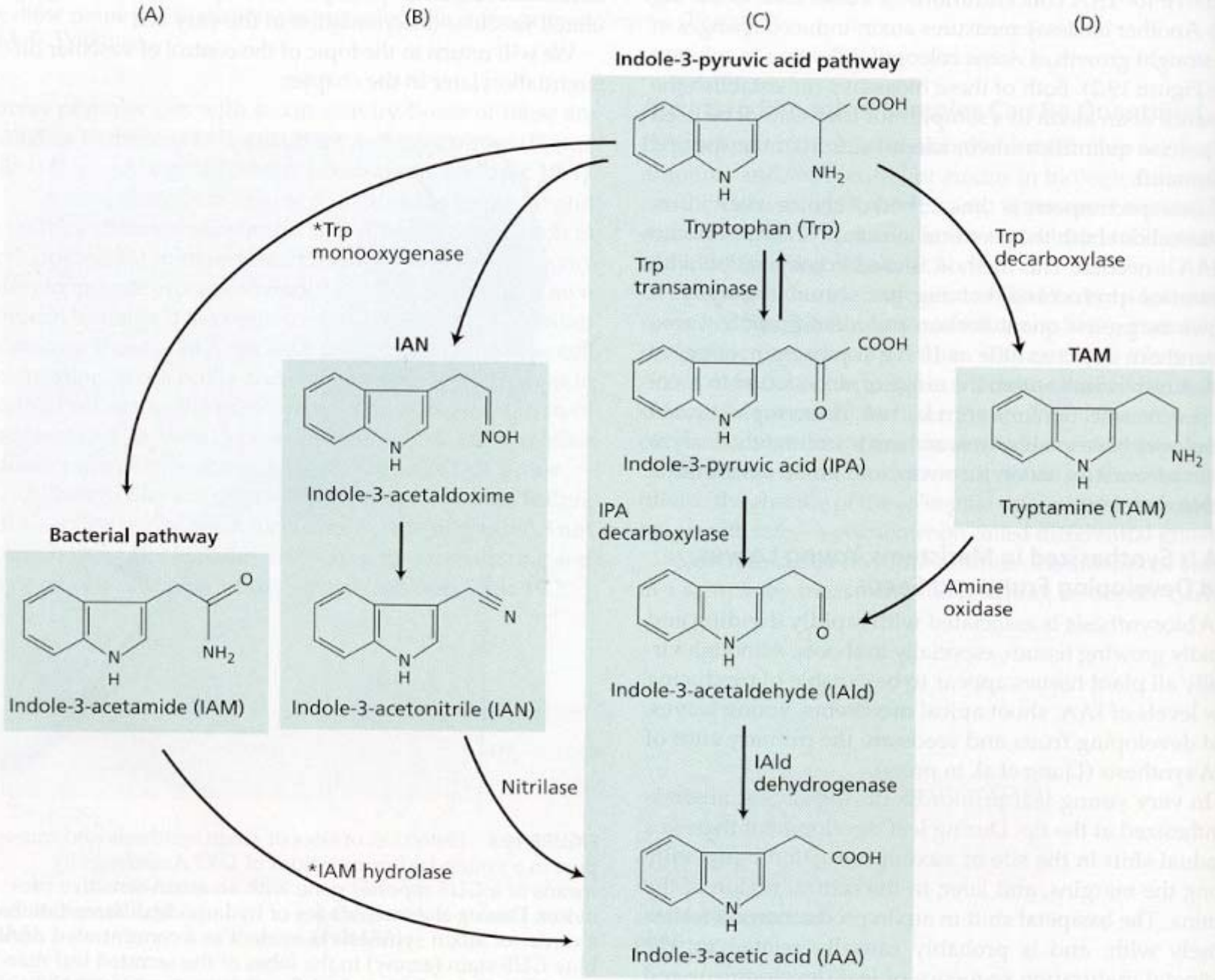

FIGURE 19.6 Tryptophan-dependent pathways of IAA biosynthesis in plants and bacteria. The enzymes that are present only in bacteria are marked with an asterisk. (After Bartel 1997.)

FIGURE 19.7 The orange pericarp (*orp*) mutant of maize is missing both subunits of tryptophan synthase. As a result, the pericarps surrounding each kernel accumulate glycosides of anthranilic acid and indole. The orange color is due to excess indole. (Courtesy of Jerry D. Cohen.)

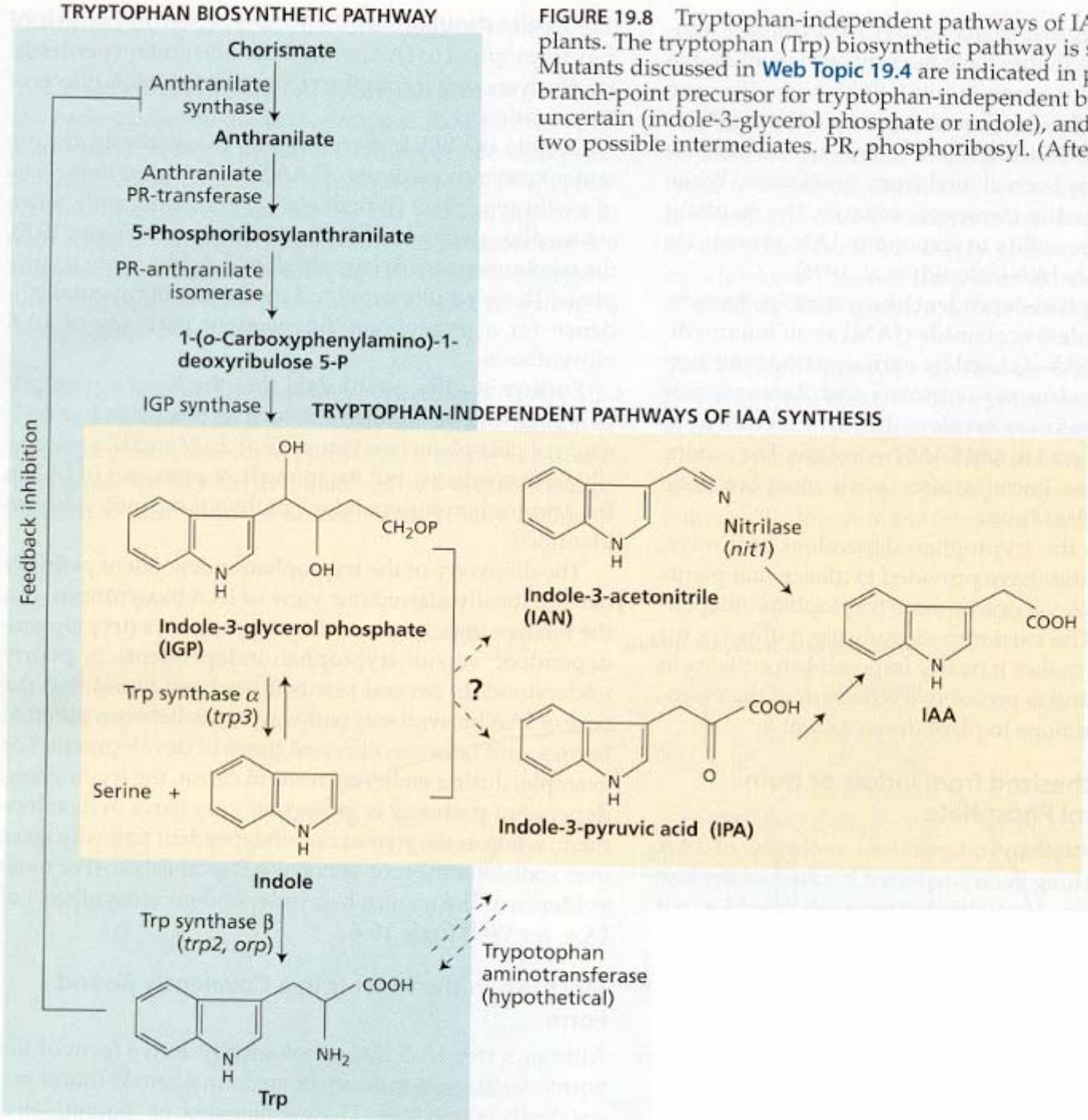

FIGURE 19.8 Tryptophan-independent pathways of IAA biosynthesis in plants. The tryptophan (Trp) biosynthetic pathway is shown on the left. Mutants discussed in **Web Topic 19.4** are indicated in parentheses. The branch-point precursor for tryptophan-independent biosynthesis is uncertain (indole-3-glycerol phosphate or indole), and IAN and IPA are two possible intermediates. PR, phosphoribosyl. (After Bartel 1997.)

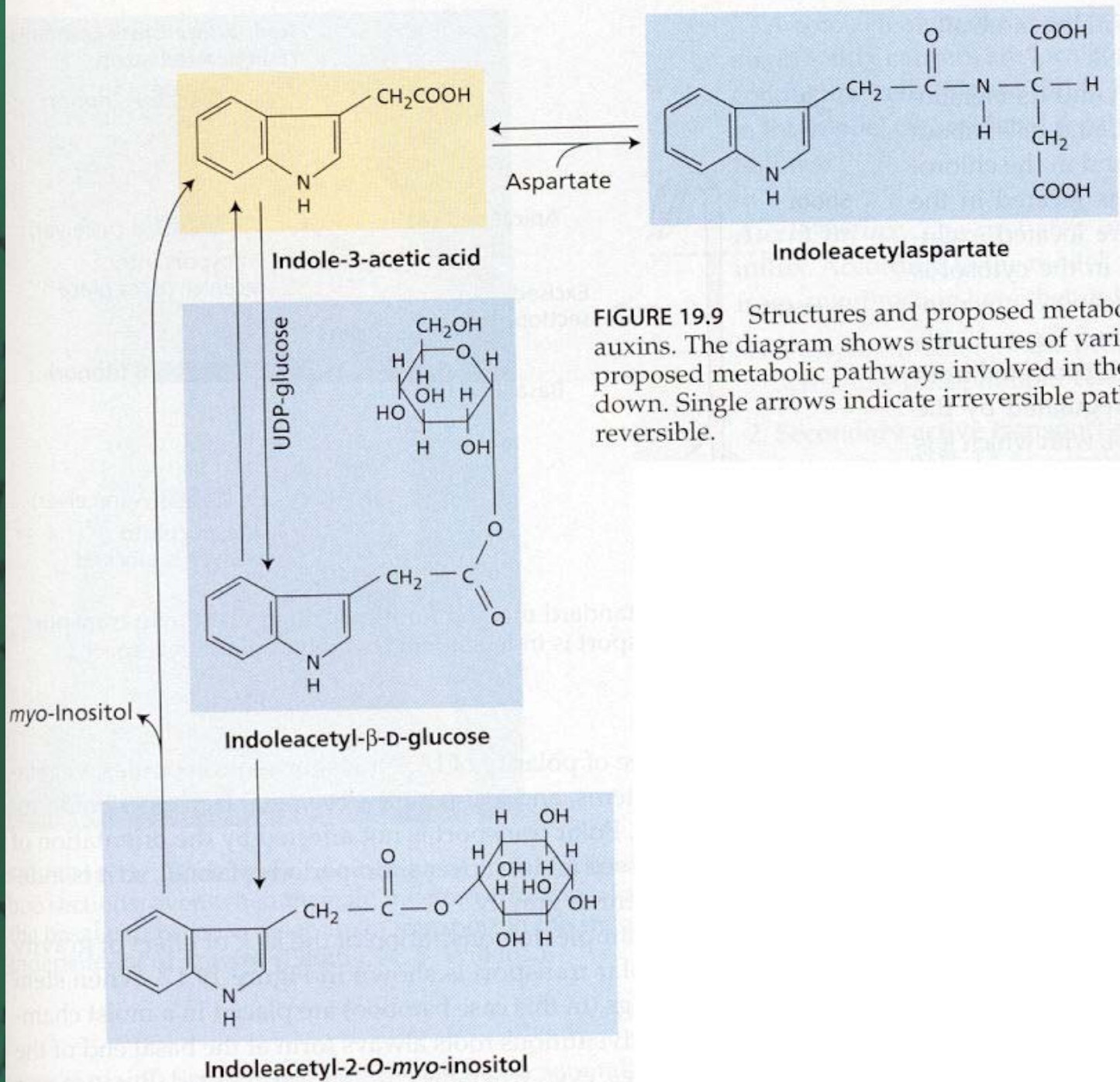

FIGURE 19.9 Structures and proposed metabolic pathways of bound auxins. The diagram shows structures of various IAA conjugates and proposed metabolic pathways involved in their synthesis and breakdown. Single arrows indicate irreversible pathways; double arrows, reversible.

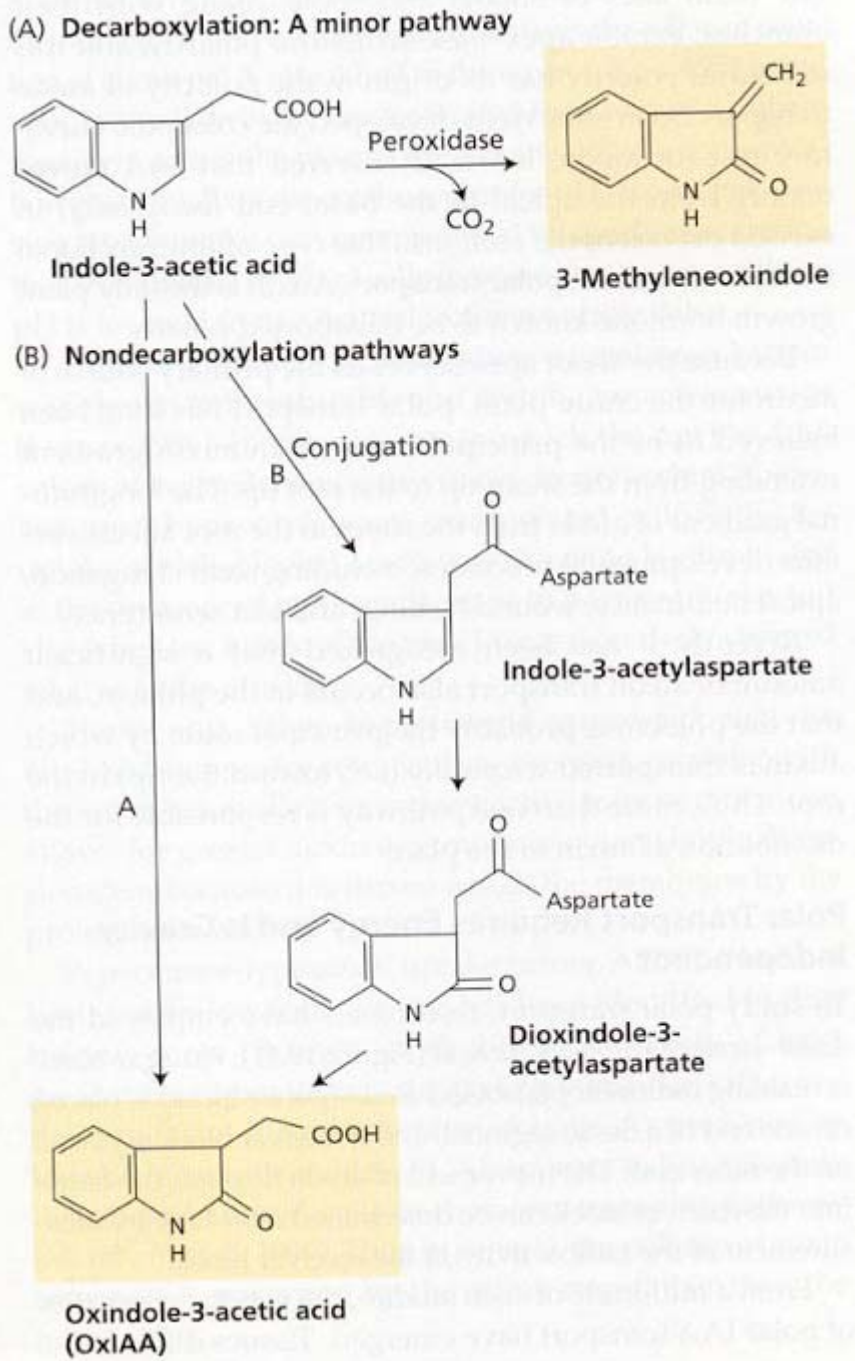

FIGURE 19.10 Biodegradation of IAA. (A) The peroxidase route (decarboxylation pathway) plays a relatively minor role. (B) The two nondecarboxylation routes of IAA oxidative degradation, A and B, are the most common metabolic pathways.

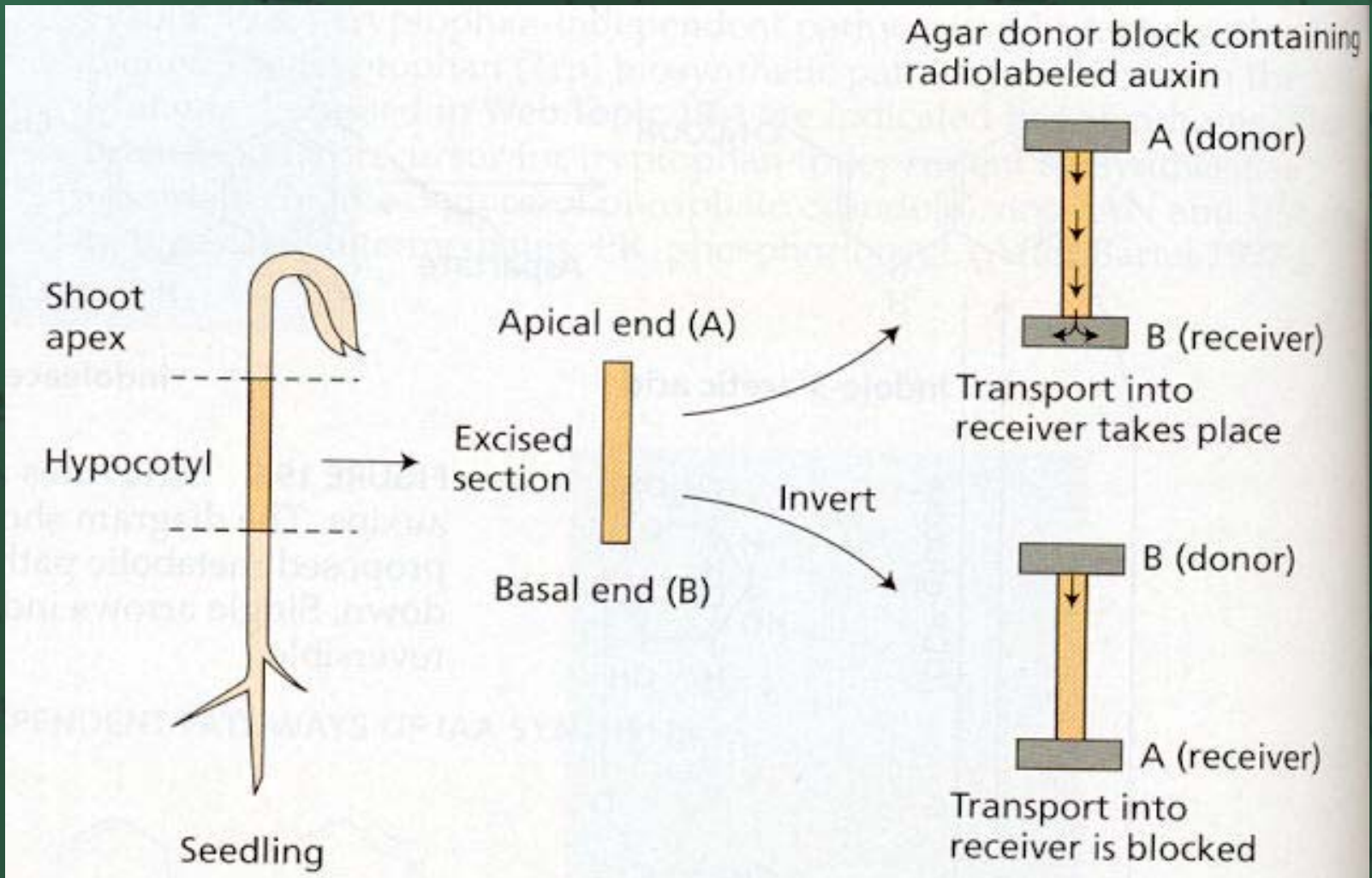

FIGURE 19.11 The standard method for measuring polar auxin transport. The polarity of transport is independent of orientation with respect to gravity.

FIGURE 19.12 Roots grow from the basal ends of these bamboo sections, even when they are inverted. The roots form at the basal end because polar auxin transport in the shoot is independent of gravity. (Photo ©M. B. Wilkins.)

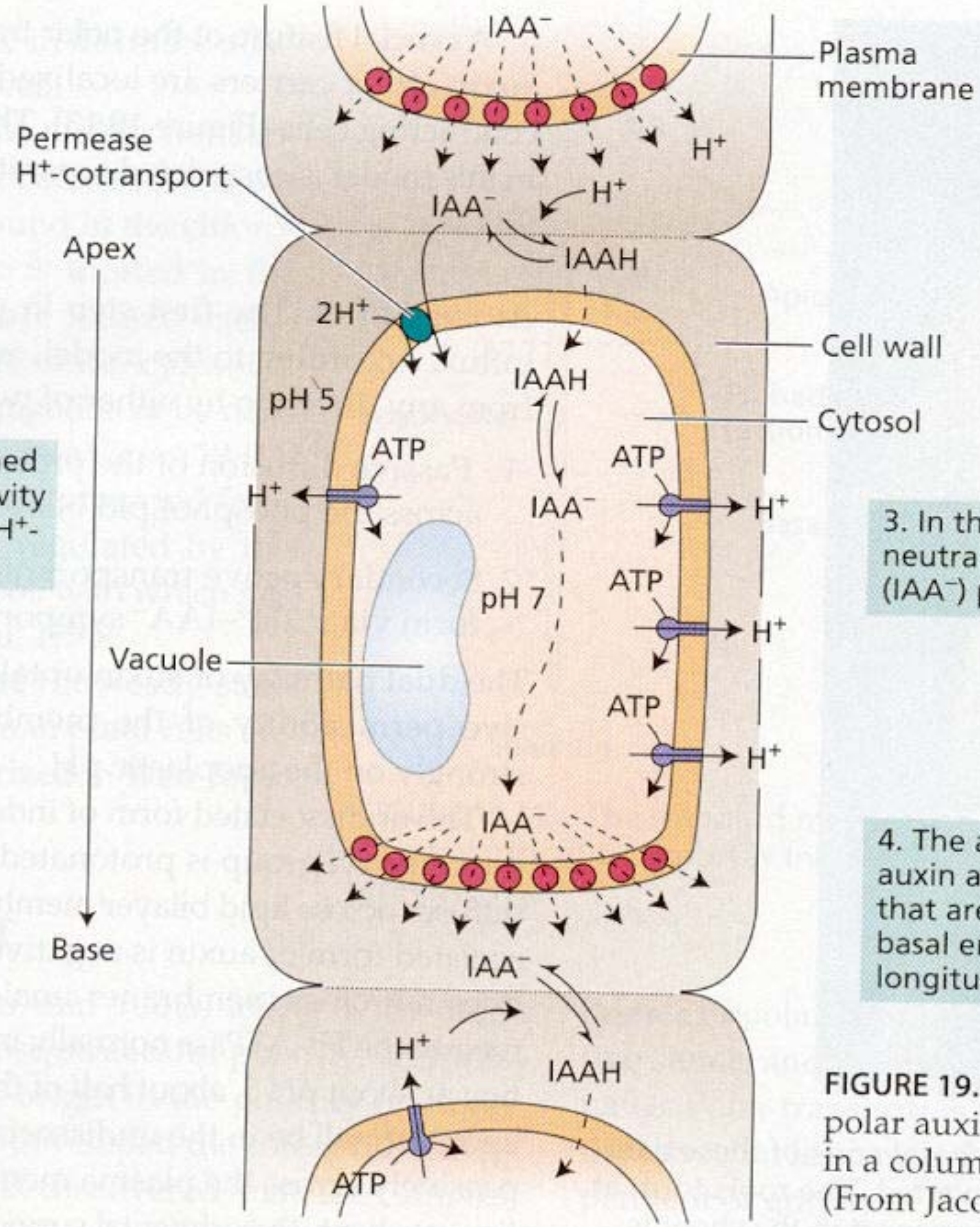

1. IAA enters the cell either passively in the undissociated form (IAAH) or by secondary active cotransport in the anionic form (IAA^-).

2. The cell wall is maintained at an acidic pH by the activity of the plasma membrane H^+-ATPase.

3. In the cytosol, which has a neutral pH, the anionic form (IAA^-) predominates.

4. The anions exit the cell via auxin anion efflux carriers that are concentrated at the basal ends of each cell in the longitudinal pathway.

FIGURE 19.13 The chemiosmotic model for polar auxin transport. Shown here is one cell in a column of auxin-transporting cells. (From Jacobs and Gilbert 1983.)

(A)

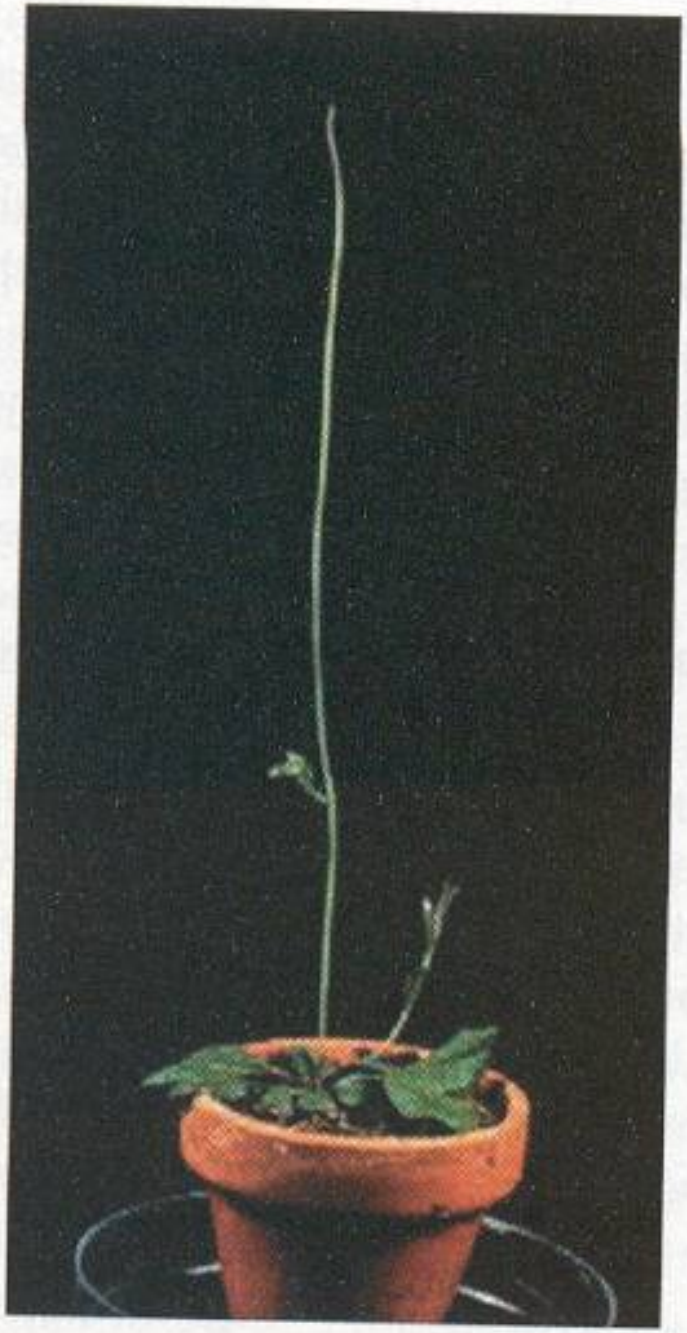

(B)

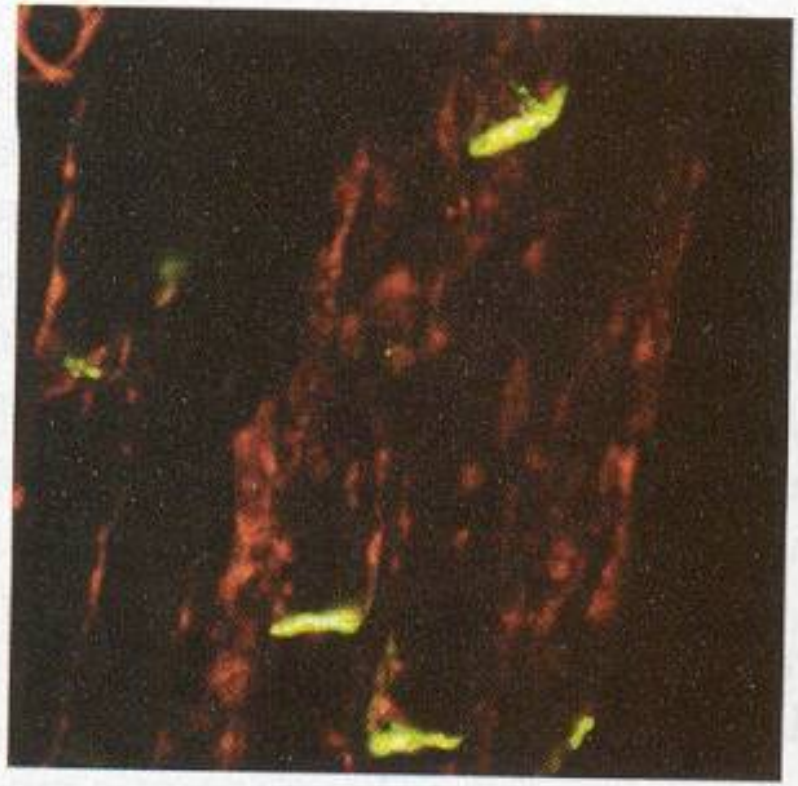

FIGURE 19.14 The *pin1* mutant of *Arabidopsis* (A) and localization of the PIN1 protein at the basal ends of conducting cells by immunofluorescence microscopy (B). (Courtesy of L. Gälweiler and K. Palme.)

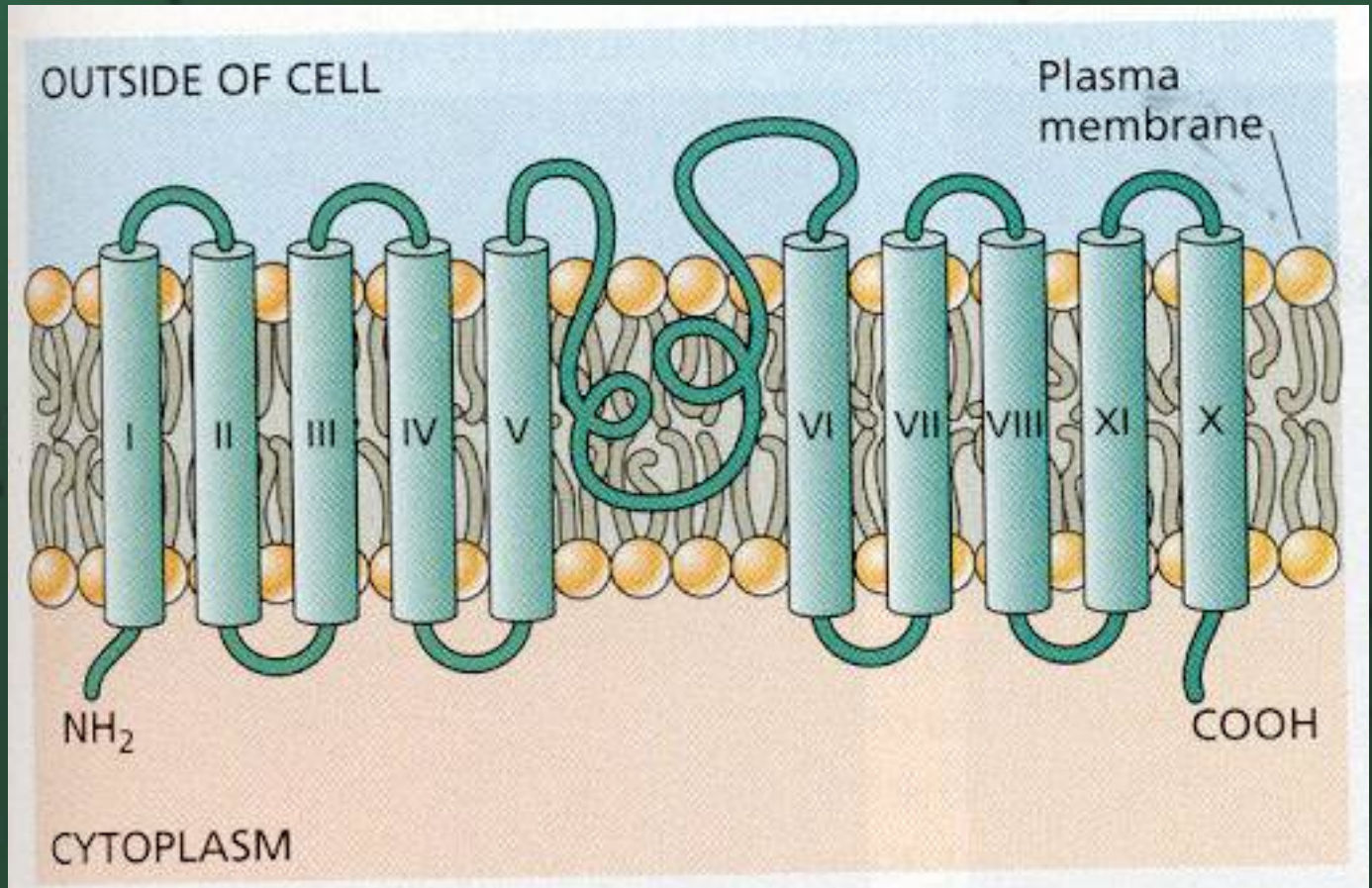

FIGURE 19.15 The topology of the PIN1 protein with ten transmembrane segments and a large hydrophilic loop in the middle. (After Palme and Gälweiler 1999.)

Auxin transport inhibitors not found in plants

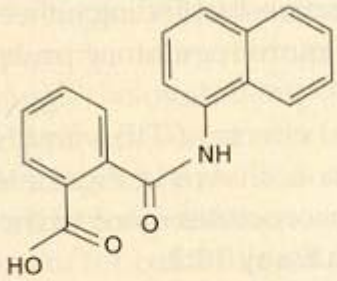

NPA (1-N-naphthylphthalamic acid)

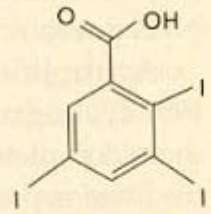

TIBA (2,3,5-triiodobenzoic acid)

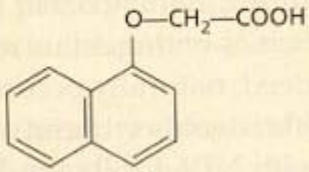

1-NOA (1-naphthoxyacetic acid)

Naturally occurring auxin transport inhibitors

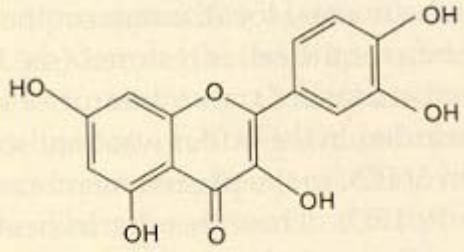

Quercetin (flavonol)

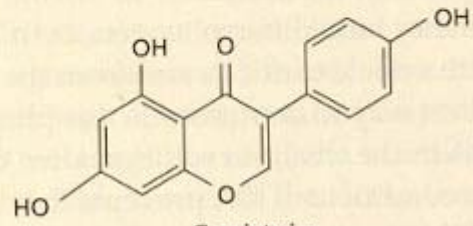

Genistein

FIGURE 19.16 Structures of auxin transport inhibitors.

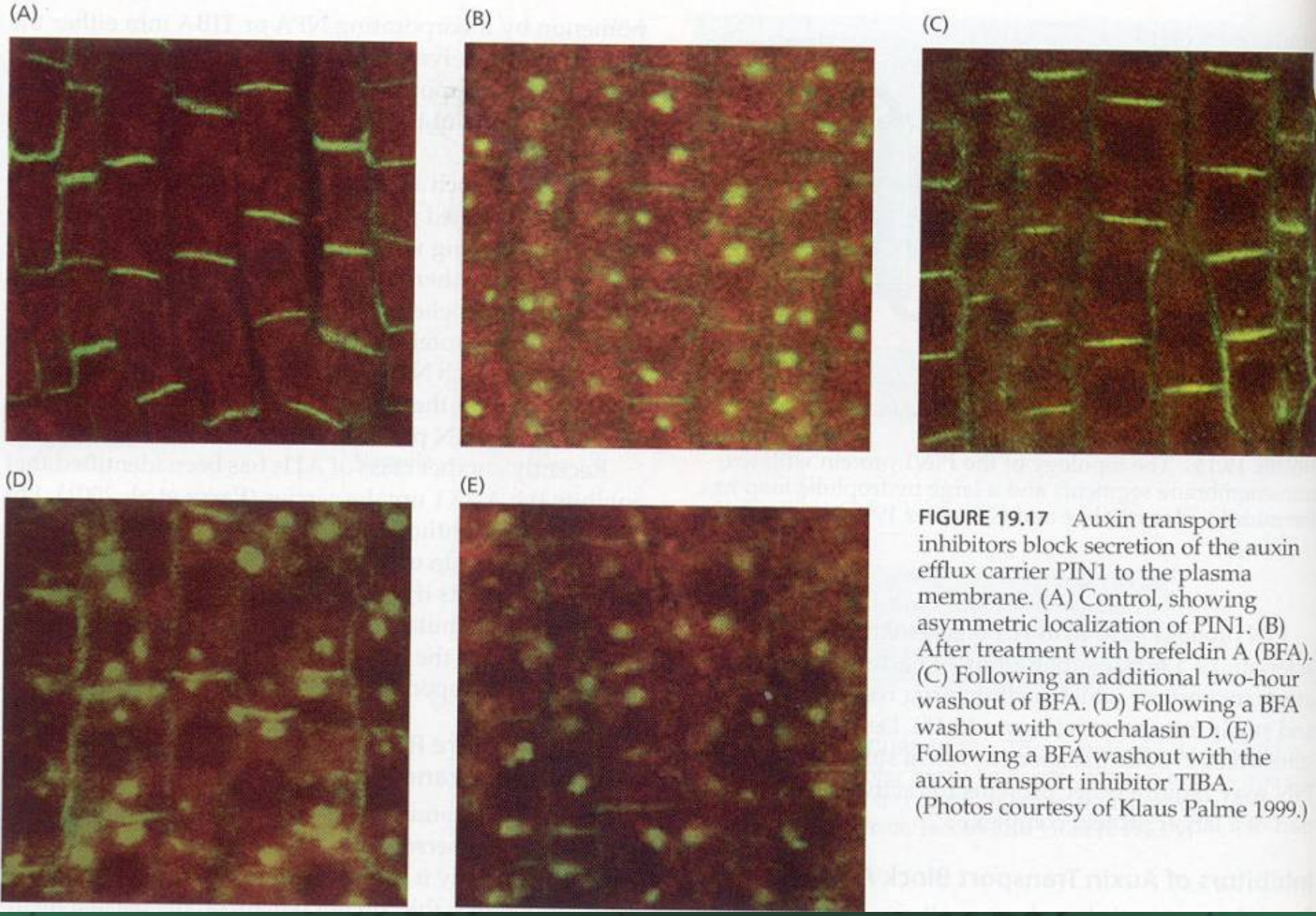

FIGURE 19.17 Auxin transport inhibitors block secretion of the auxin efflux carrier PIN1 to the plasma membrane. (A) Control, showing asymmetric localization of PIN1. (B) After treatment with brefeldin A (BFA). (C) Following an additional two-hour washout of BFA. (D) Following a BFA washout with cytochalasin D. (E) Following a BFA washout with the auxin transport inhibitor TIBA. (Photos courtesy of Klaus Palme 1999.)

FIGURE 19.18 Actin-dependent PIN cycling between the plasma membrane and an endosomal compartment. Auxin transport inhibitors TIBA and NPA both interfere with relocalization of PIN1 proteins to basal plasma membranes after BFA washout (see Figure 19.17). This suggests that both of these auxin transport inhibitors interfere with PIN1 cycling.

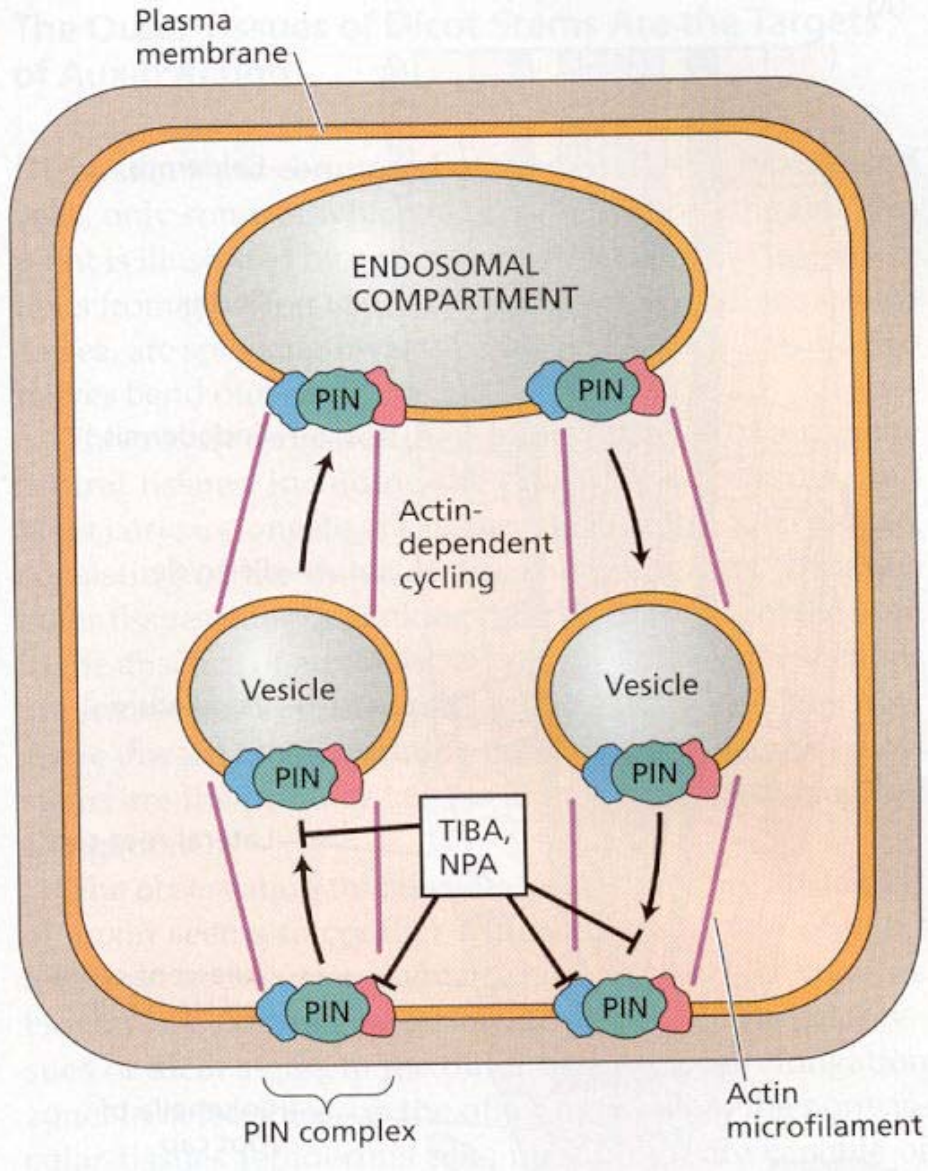

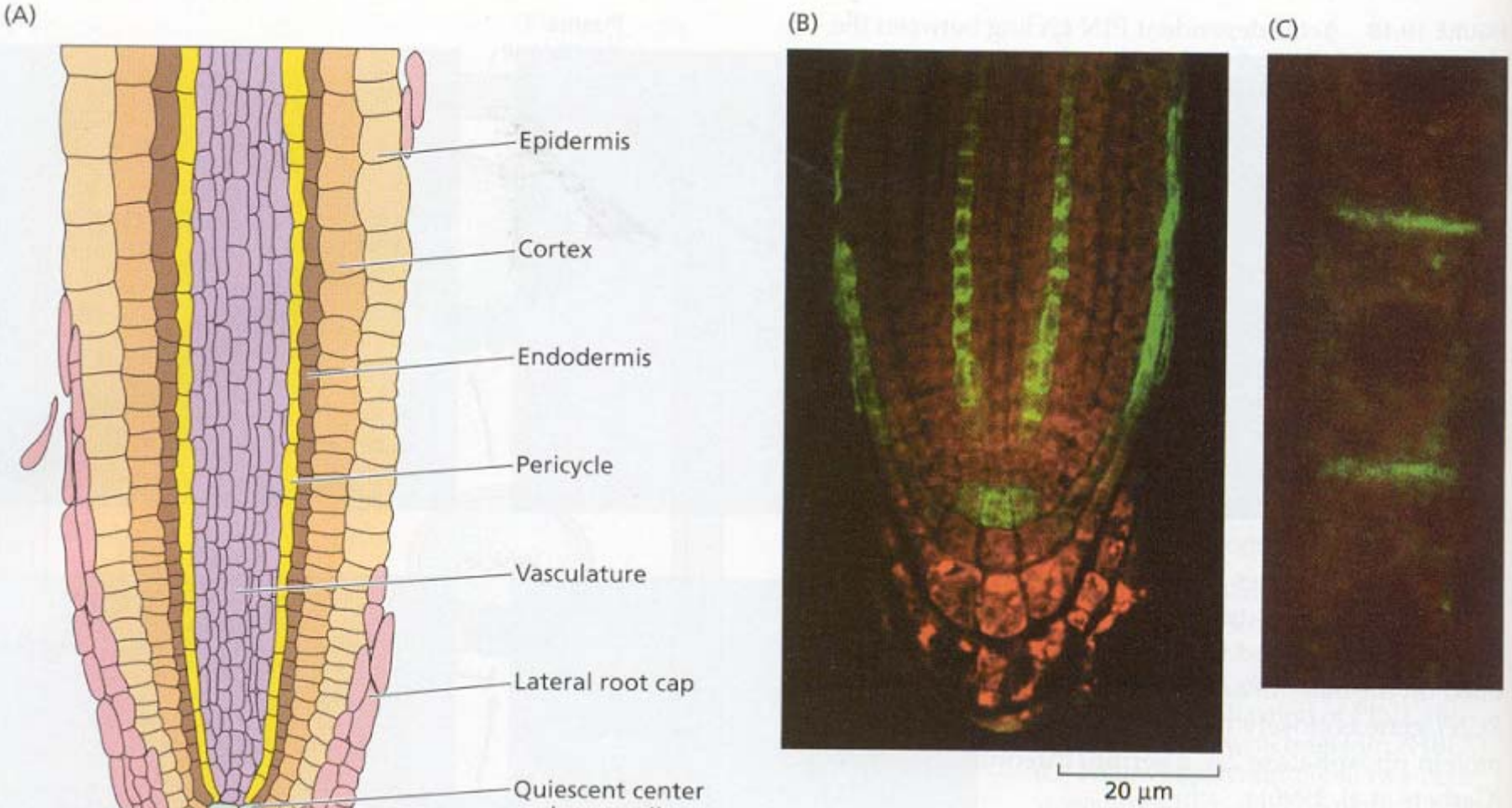

FIGURE 19.19 The auxin permease AUX1 is specifically expressed in a subset of columella, lateral root cap, and stellar tissues. (A) Diagram of tissues in the *Arabidopsis* root tip. (B) Immunolocalization of AUX1 in protophloem cells of the stele, a central cluster of cells in the columella, and lateral root cap cells. (C) Asymmetric localization of AUX1 in a file of protophloem cells. Scale bar is 2 μm in C. (From Swarup et al. 2001.)

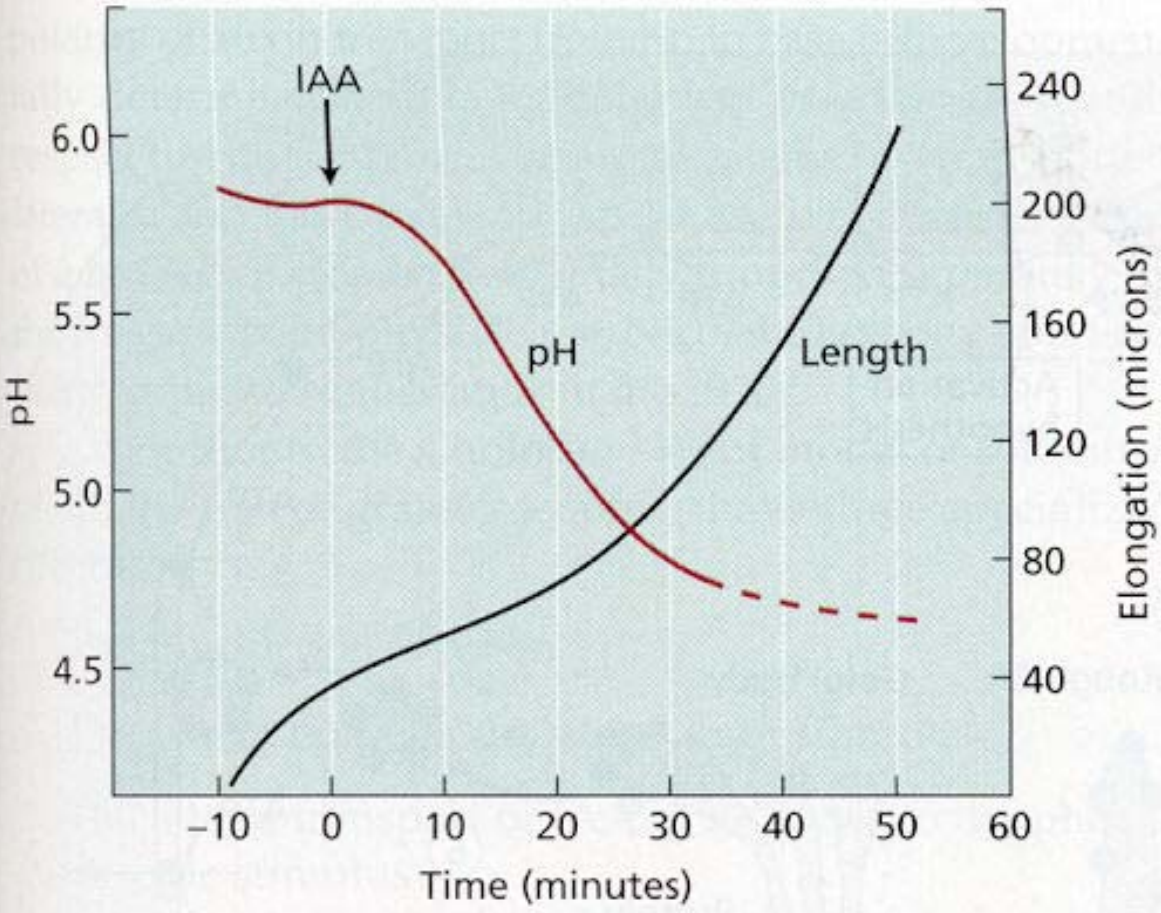

FIGURE 19.23 Kinetics of auxin-induced elongation and cell wall acidification in maize coleoptiles. The pH of the cell wall was measured with a pH microelectrode. Note the similar lag times (10 to 15 minutes) for both cell wall acidification and the increase in the rate of elongation. (From Jacobs and Ray 1976.)

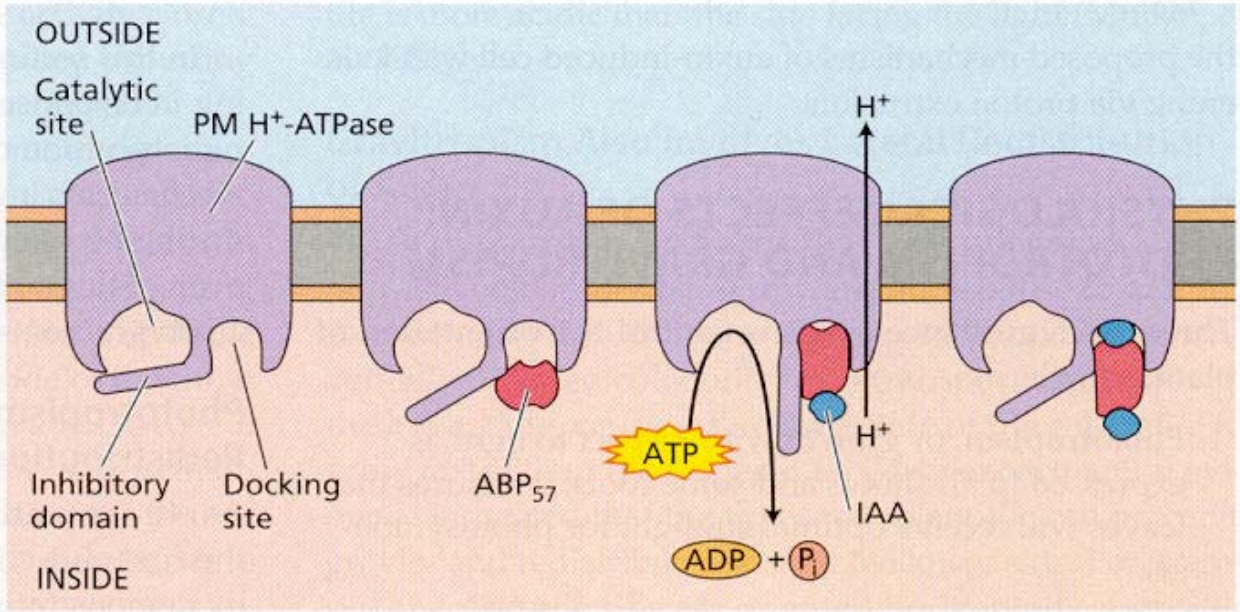

FIGURE 19.24 Model for the activation of the plasma membrane (PM) H^+-ATPase by ABP_{57} and auxin.

Activation hypothesis: Auxin binds to an auxin-binding protein (ABP1) located either on the cell surface or in the cytosol. ABP1-IAA then interacts directly with plasma membrane H^+-ATPase to stimulate proton pumping (step 1). Second messengers, such as calcium or intracellular pH, could also be involved.

Synthesis hypothesis: IAA-induced second messengers activate the expression of genes (step 2) that encode the plasma membrane H^+-ATPase (step 3). The protein is synthesized on the rough endoplasmic reticulum (step 4) and targeted via the secretory pathway to the plasma membrane (steps 5 and 6). The increase in proton extrusion results from an increase in the number of proton pumps on the membrane.

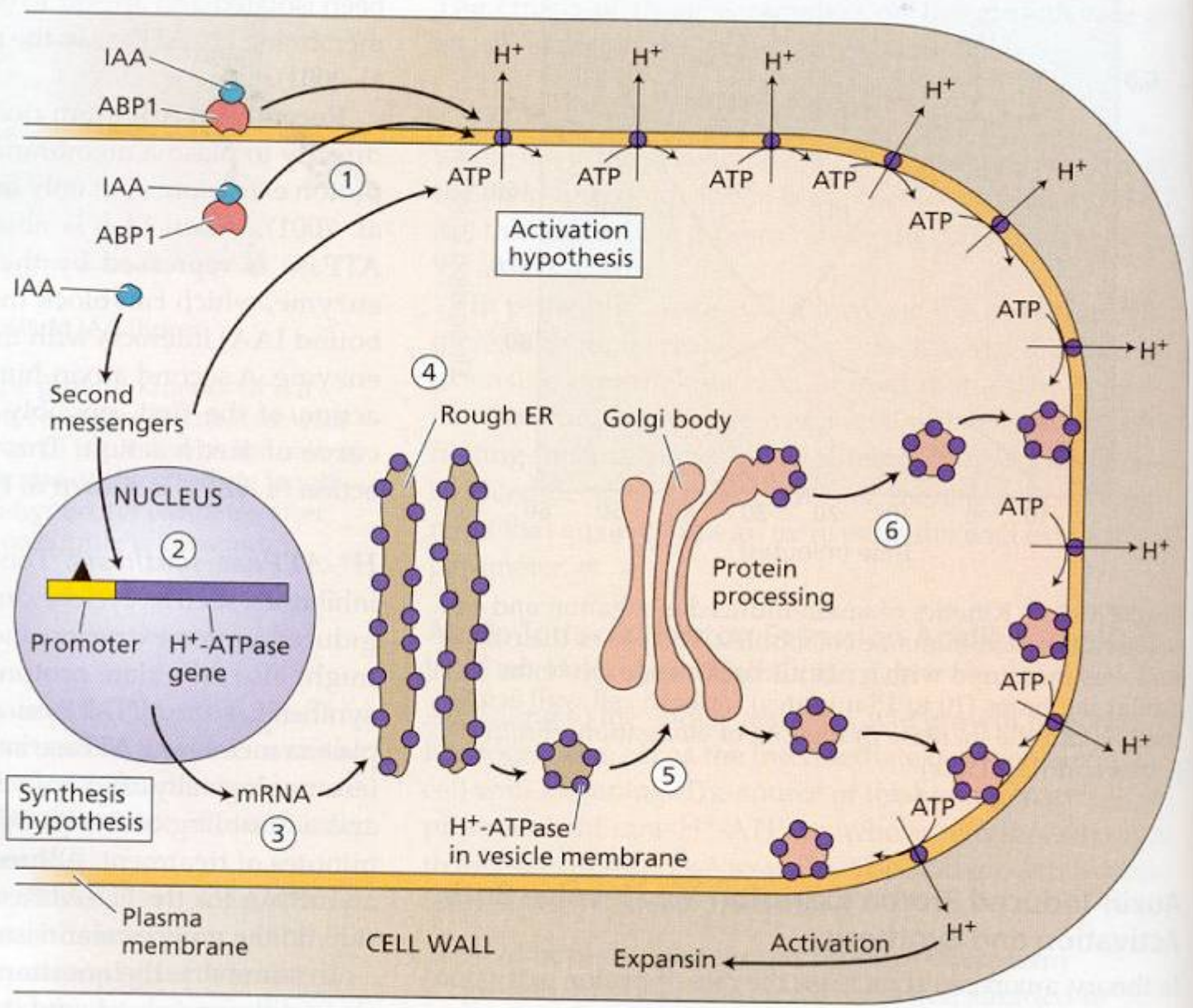

FIGURE 19.25 Current models for IAA-induced H^+ extrusion. In many plants, both of these mechanisms may operate. Regardless of how H^+ pumping is increased, acid-induced wall loosening is thought to be mediated by expansins.

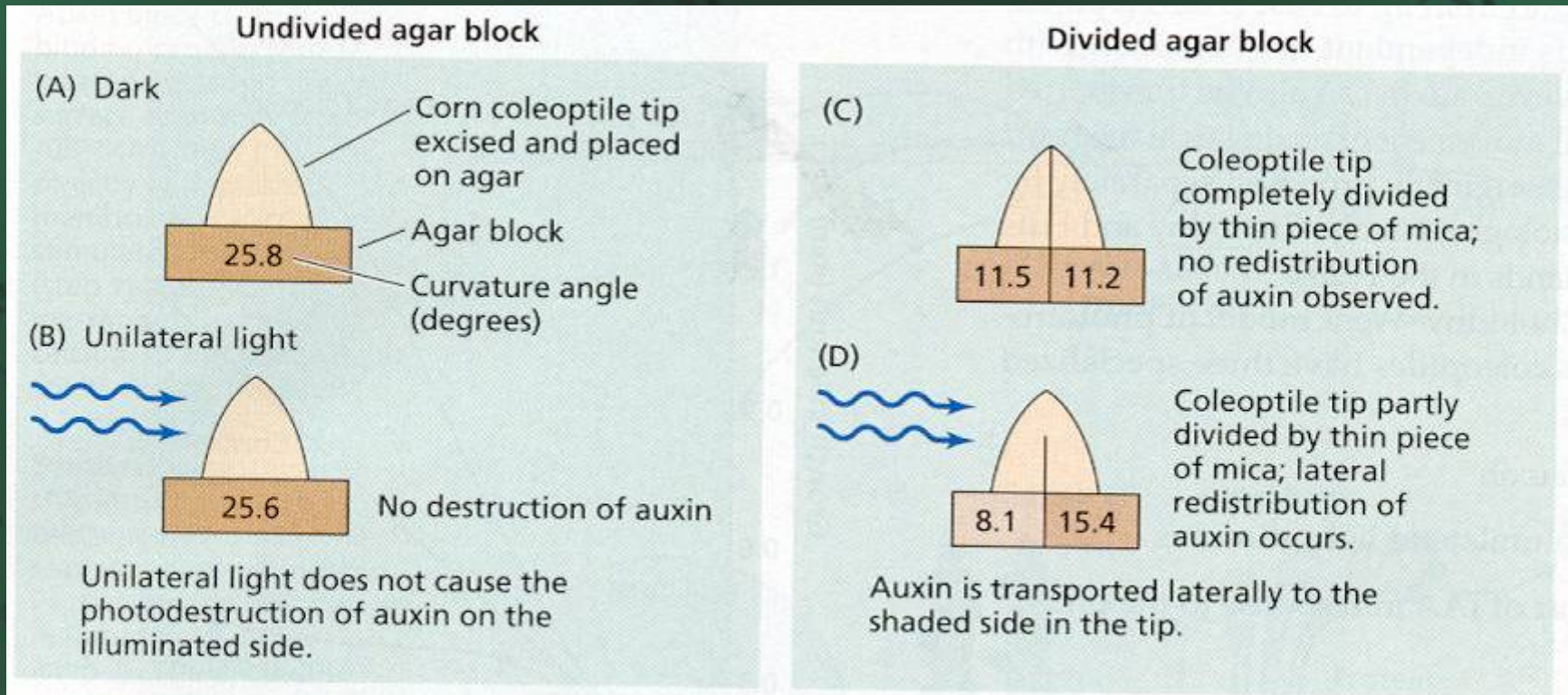

FIGURE 19.27 Evidence that the lateral redistribution of auxin is stimulated by unidirectional light in corn coleoptiles.

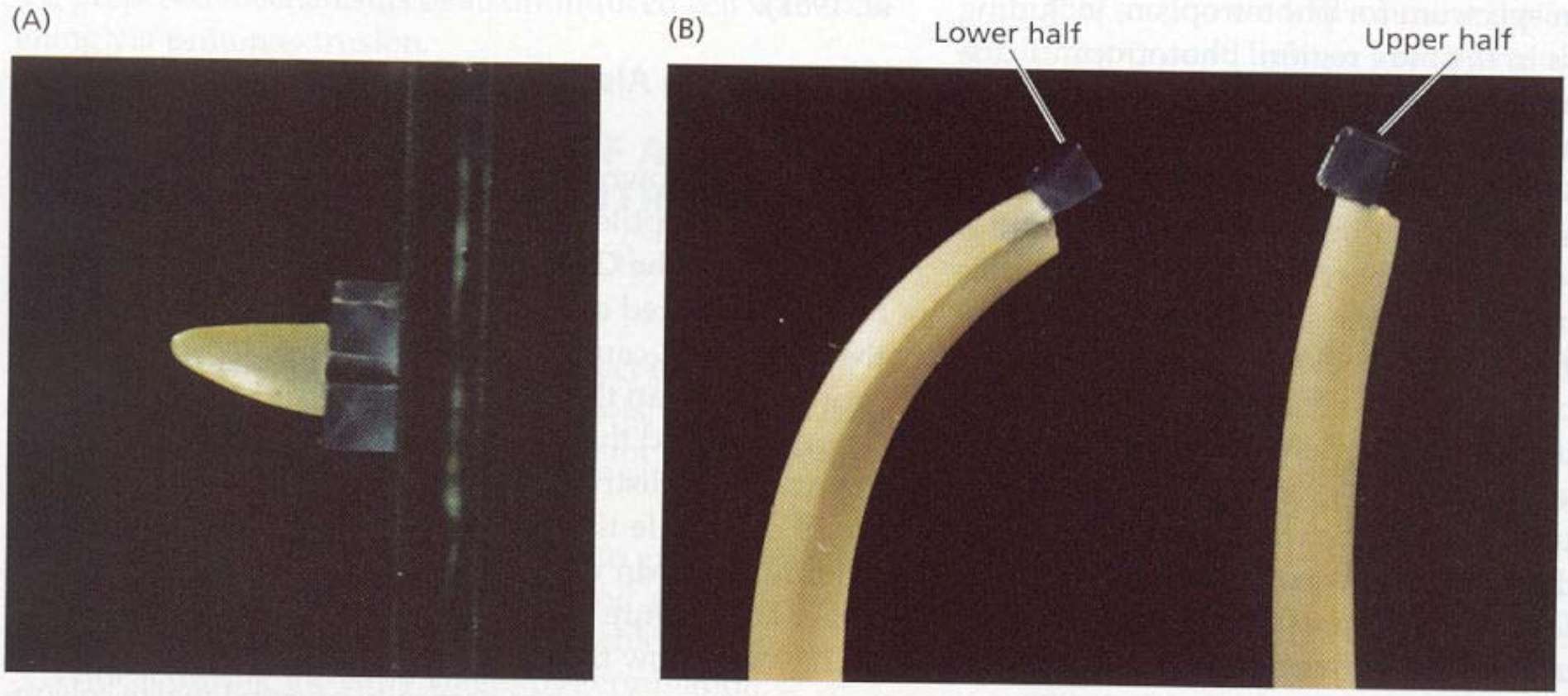

FIGURE 19.28 Auxin is transported to the lower side of a horizontally oriented oat coleoptile tip. (A) Auxin from the upper and lower halves of a horizontal tip is allowed to diffuse into two agar blocks. (B) The agar block from the lower half (left) induces greater curvature in a decapitated coleoptile than the agar block from the upper half (right). (Photo © M. B. Wilkins.)

FIGURE 19.29 Lateral auxin gradients are formed in *Arabidopsis* hypocotyls during the differential growth responses to light (A) and gravity (B). The plants were transformed with the *DR5::GUS* reporter gene. Auxin accumulation on the shaded (A) or lower (B) side of the hypocotyls is indicated by the blue staining shown in the insets. (Photos courtesy of Klaus Palme.)

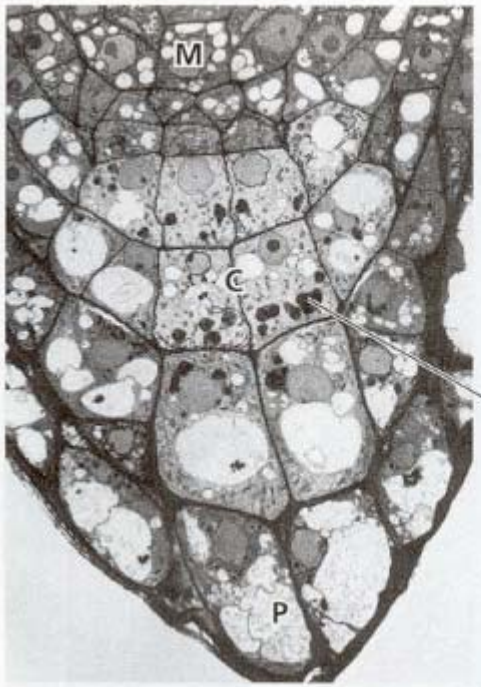

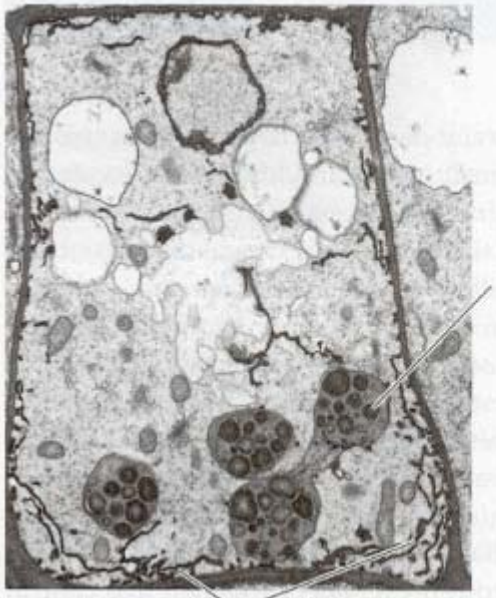

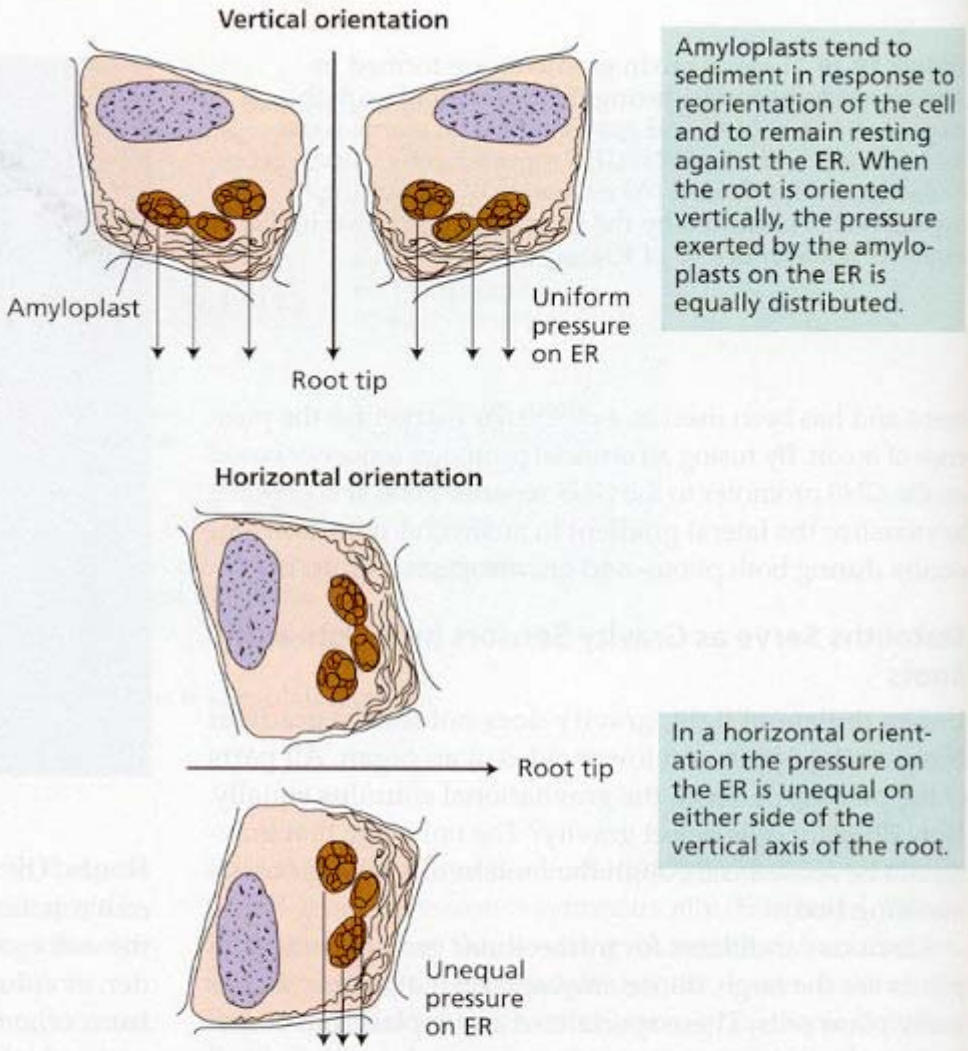

FIGURE 19.30 The perception of gravity by statocytes of *Arabidopsis*. (A) Electron micrograph of root tip, showing apical meristem (M), columella (C), and peripheral (P) cells. (B) Enlarged view of a columella cell, showing the amyloplasts resting on top of endoplasmic reticulum at the bottom of the cell. (C) Diagram of the changes that occur during reorientation from the vertical to the horizontal position. (A, B courtesy of Dr. John Kiss; C based on Sievers et al. 1996 and Volkmann and Sievers 1979.)

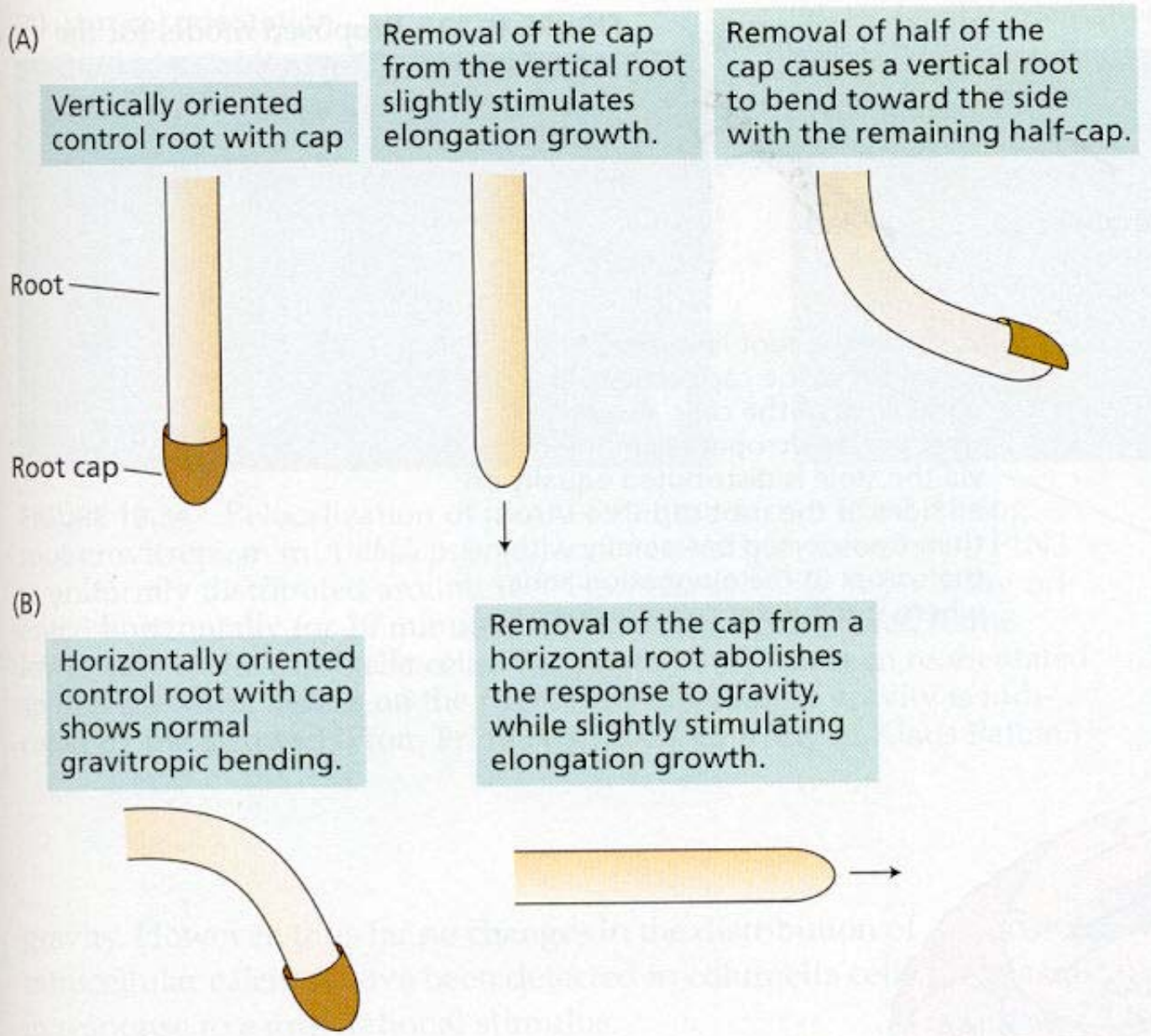

FIGURE 19.31 Microsurgery experiments demonstrating that the root cap produces an inhibitor that regulates root gravitropism. (After Shaw and Wilkins 1973.)

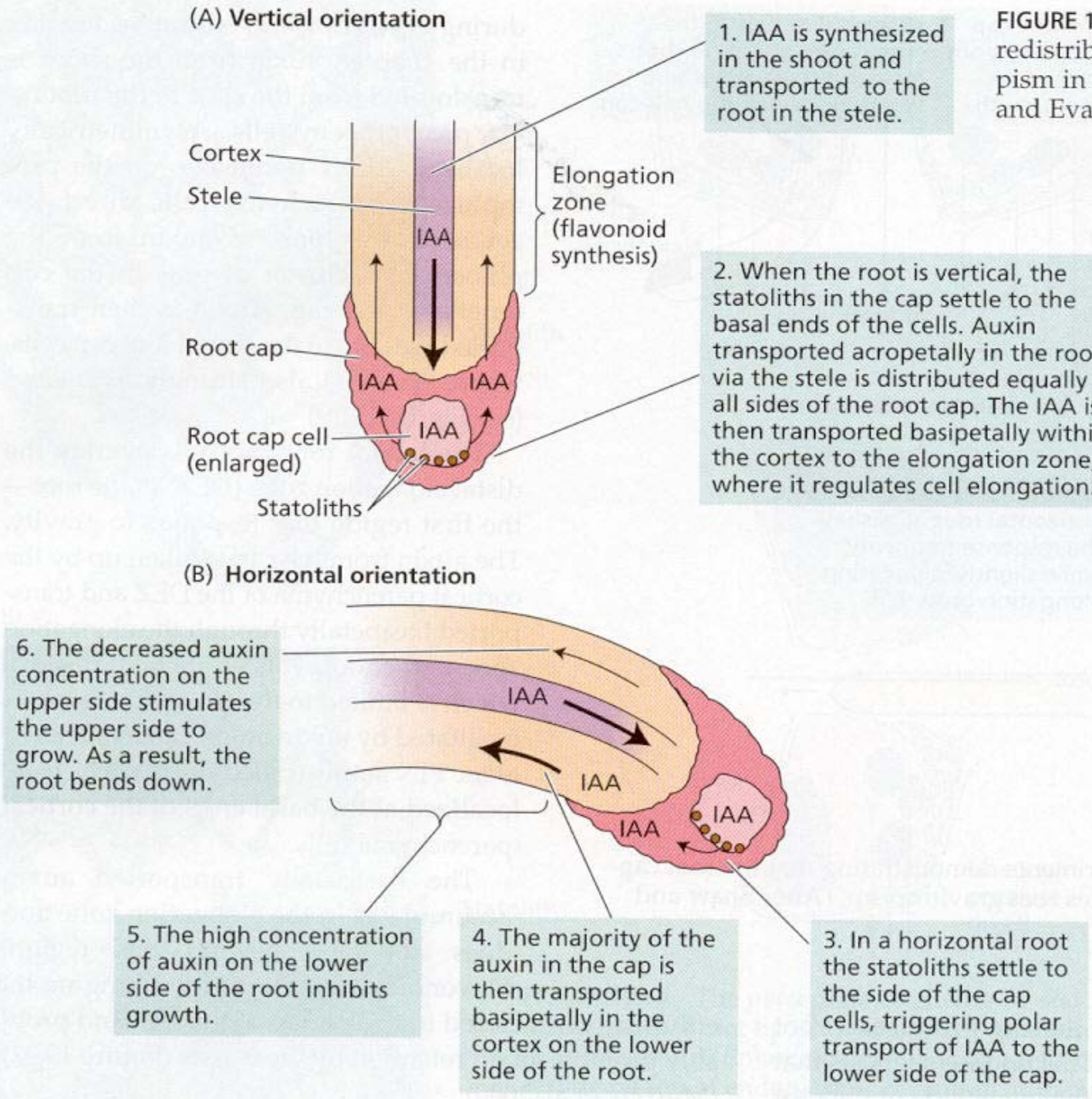

FIGURE 19.33 Proposed model for the redistribution of auxin during gravitropism in maize roots. (After Hasenstein and Evans 1988.)

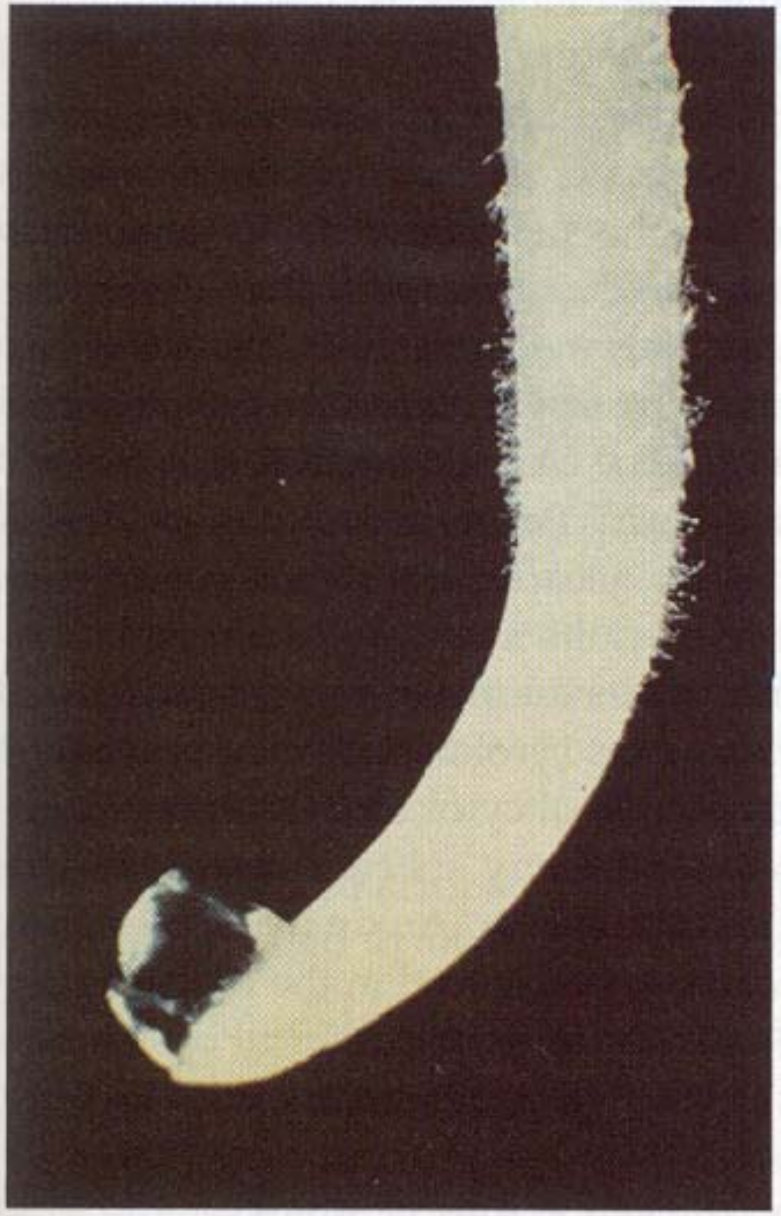

FIGURE 19.35 A corn root bending toward an agar block containing calcium placed on the cap. (Courtesy of Michael L. Evans.)

FIGURE 19.36 Auxin suppresses the growth of axillary buds in bean (*Phaseolus vulgaris*) plants. (A) The axillary buds are suppressed in the intact plant because of apical dominance. (B) Removal of the terminal bud releases the axillary buds from apical dominance (arrows). (C) Applying IAA in lanolin paste (contained in the gelatin capsule) to the cut surface prevents the outgrowth of the axillary buds. (Photos ©M. B. Wilkins.)

(A)

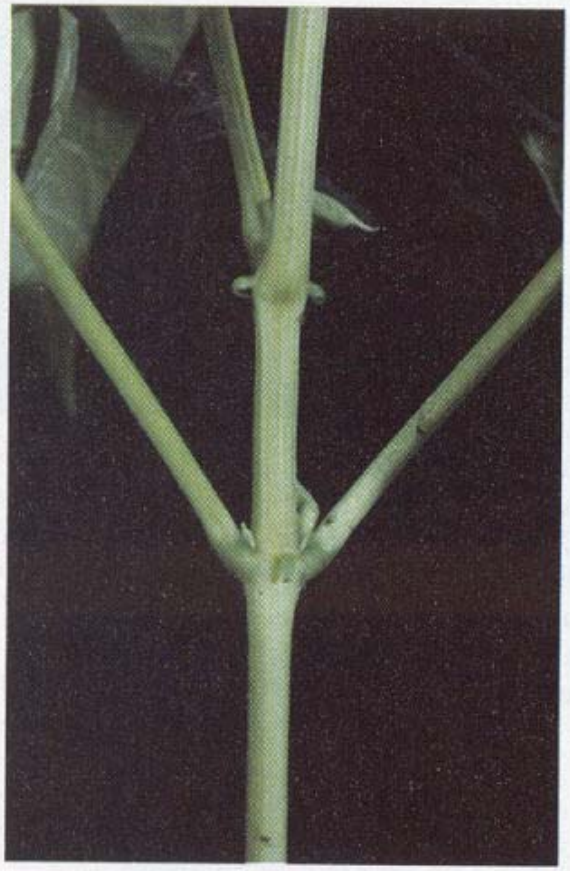

(B)

(C)

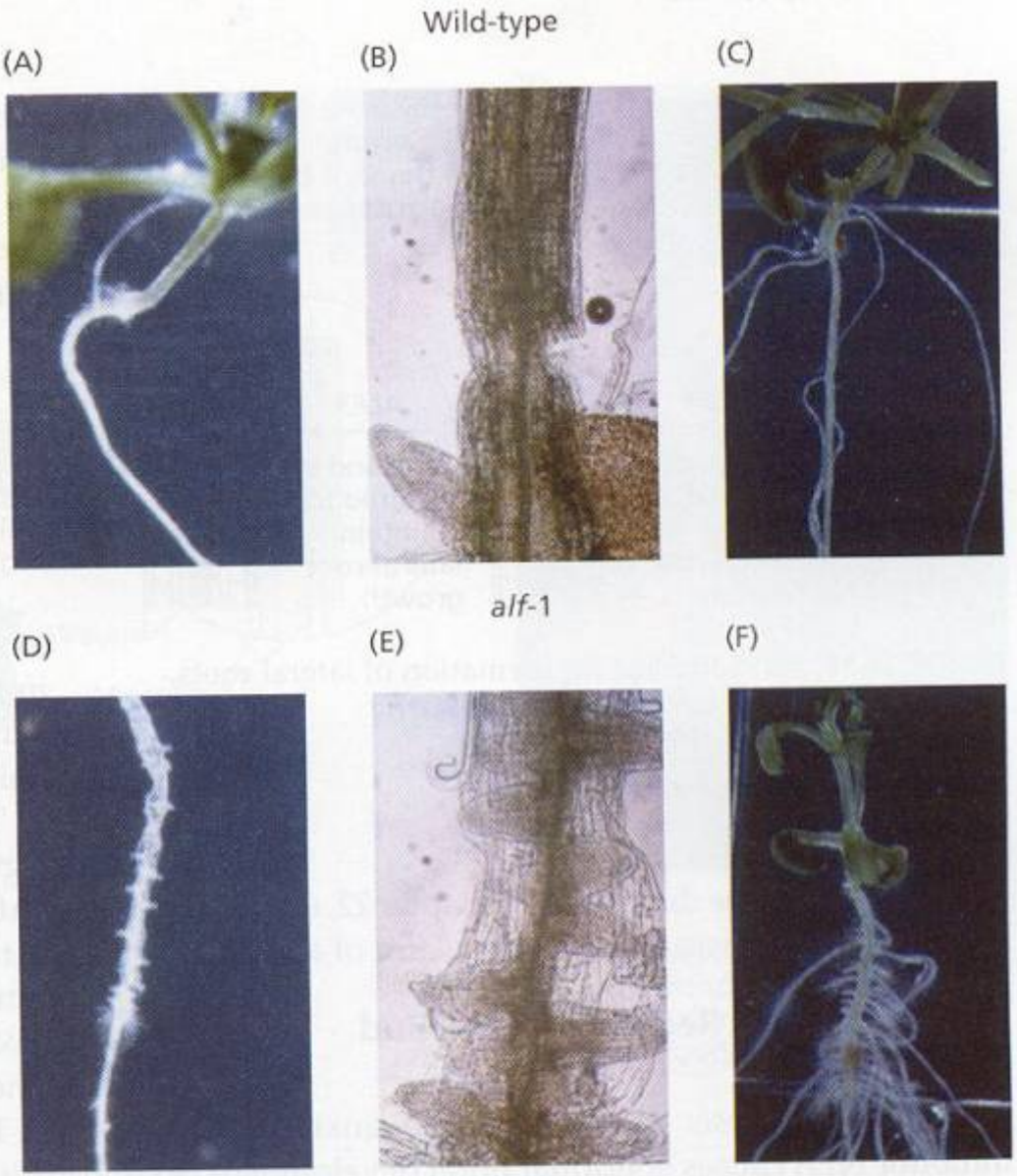

FIGURE 19.37 Root morphology of *Arabidopsis* (A–C) wild-type and *alf1* seedlings (D–F) on hormone-free medium. Note the proliferation of root primoridia growing from the pericycle in the *alf1* seedlings (D and E). (From Celenza et al. 1995, courtesy of J. Celenza.)

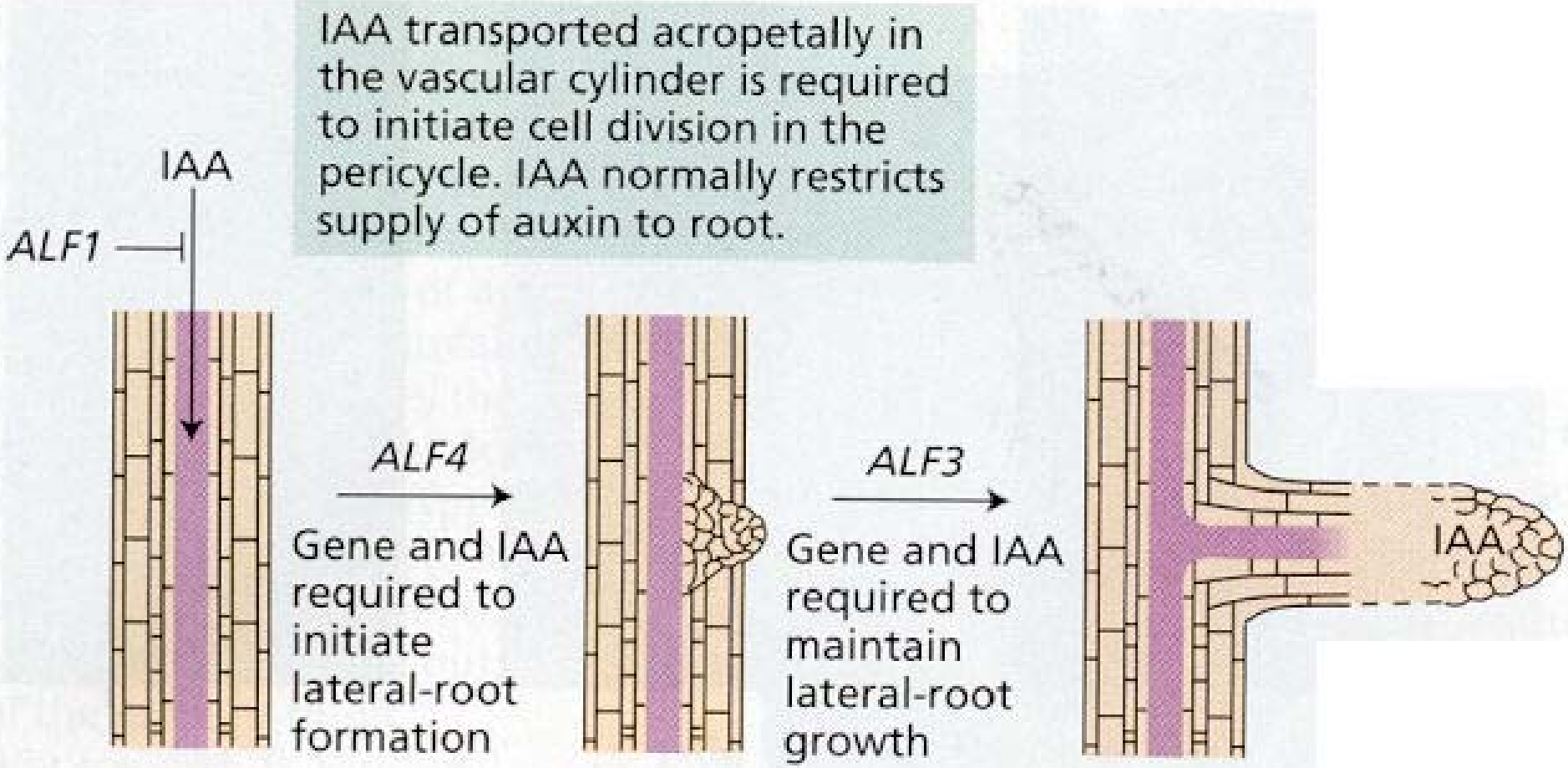

FIGURE 19.38 A model for the formation of lateral roots, based on the *alf* mutants of *Arabidopsis*. (After Celenza et al. 1995.)

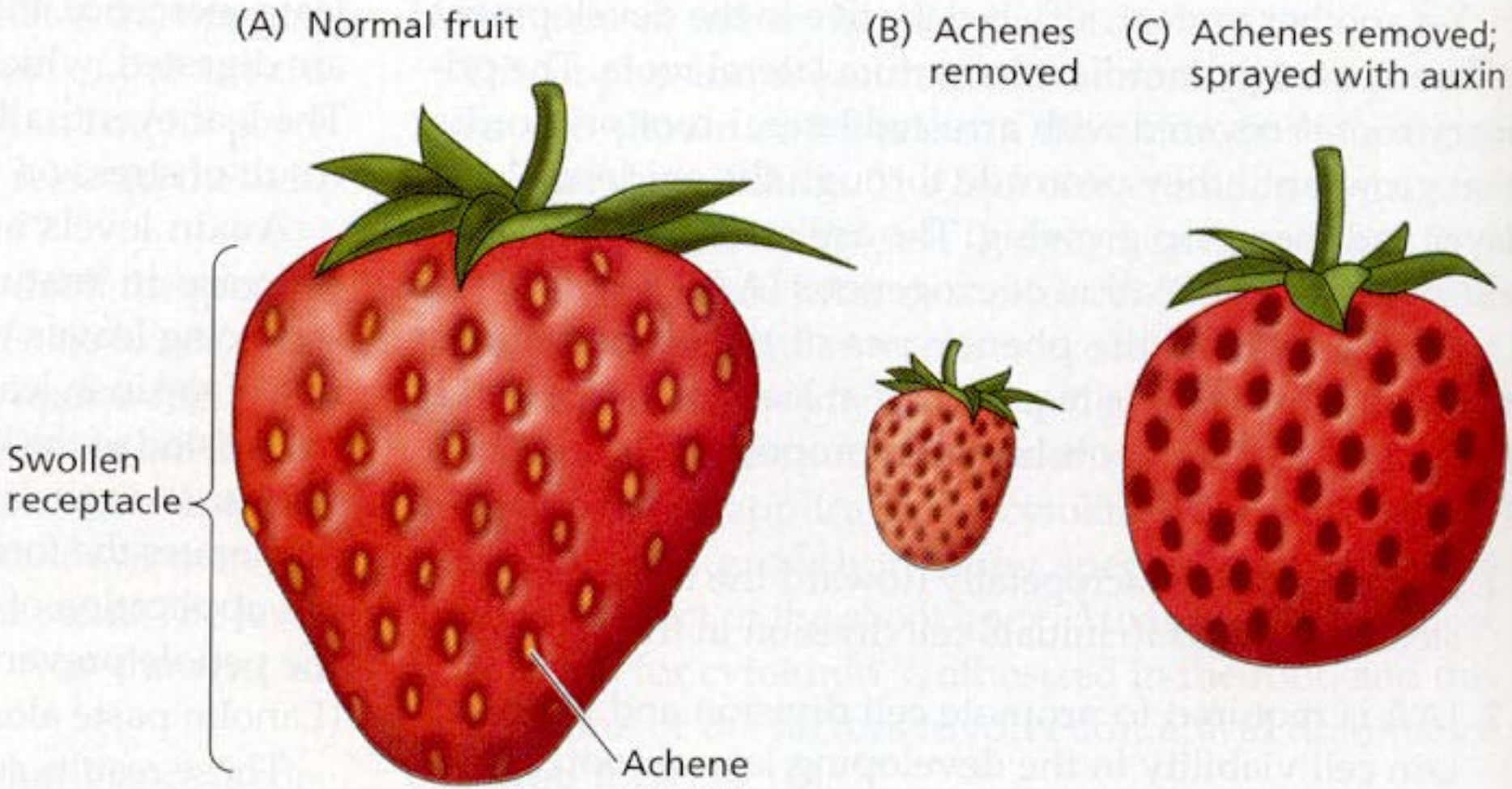

FIGURE 19.39 (A) The strawberry "fruit" is actually a swollen receptacle whose growth is regulated by auxin produced by the "seeds," which are actually achenes–the true fruits. (B) When the achenes are removed, the receptacle fails to develop normally. (C) Spraying the achene-less receptacle with IAA restores normal growth and development. (After A. Galston 1994.)

(A)

The stem was decapitated, and the leaves and buds above the wound site were removed to lower the endogenous auxin.

Immediately after the wounding, IAA in lanolin paste was applied to the stem above the wound.

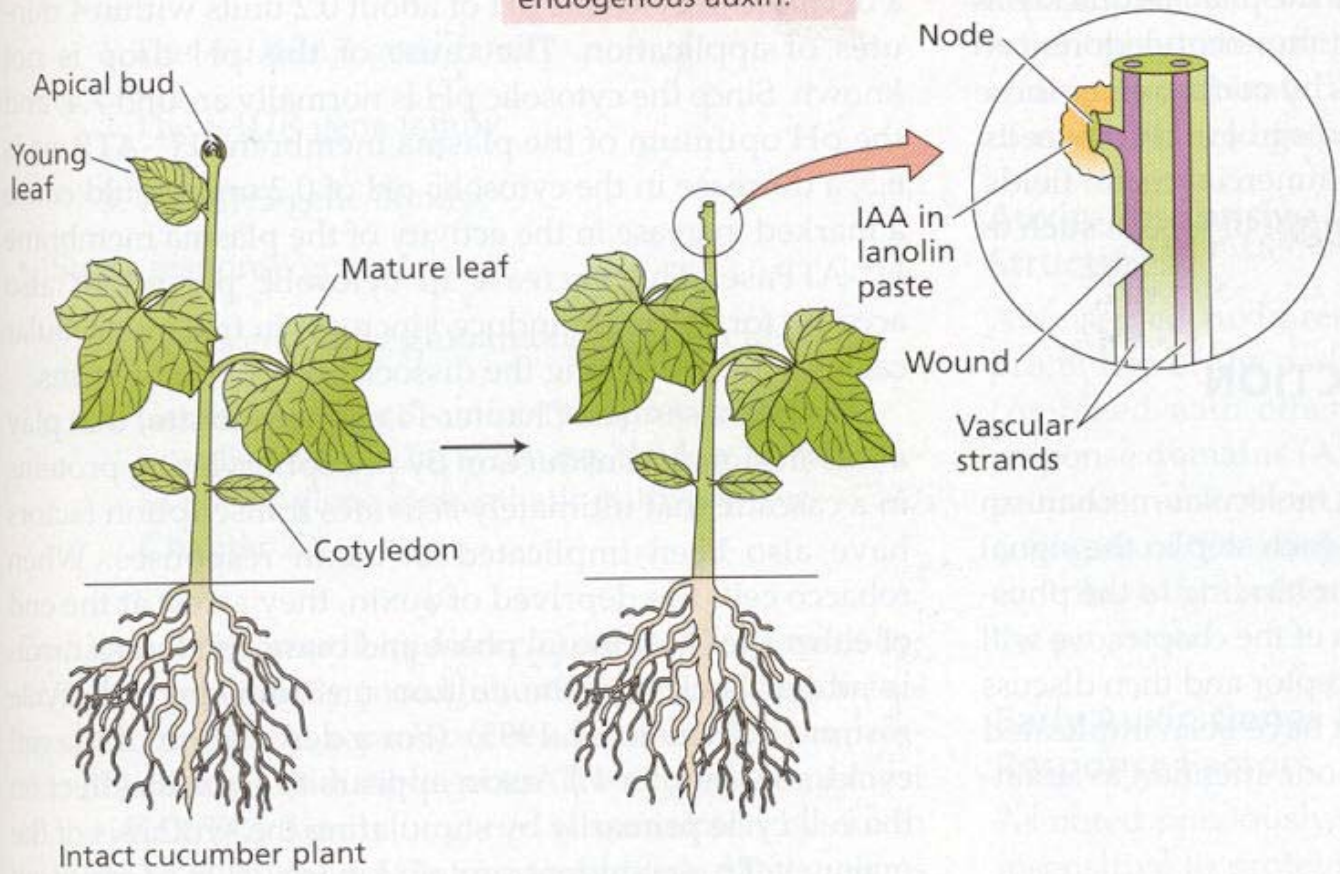

(B)

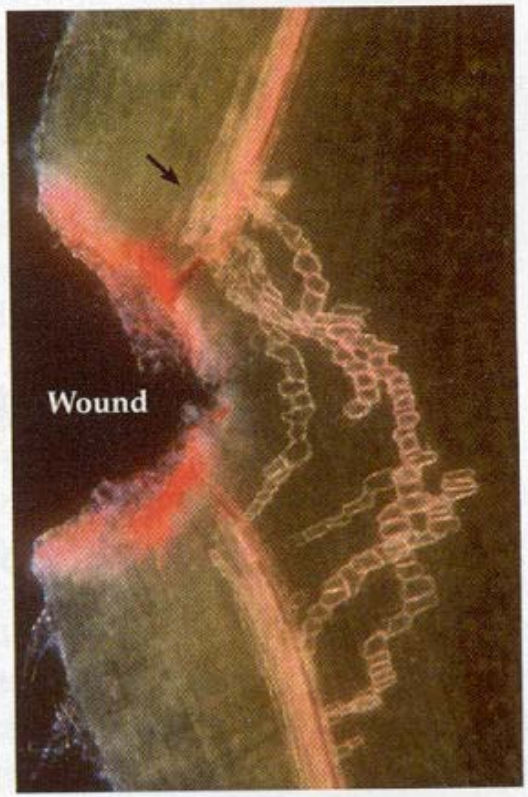

Xylem differentiation occurs around the wound, following the path of auxin diffusion.

FIGURE 19.40 IAA-induced xylem regeneration around the wound in cucumber (*Cucumis sativus*) stem tissue. (A) Method for carrying out the wound regeneration experiment. (B) Fluorescence micrograph showing regenerating vascular tissue around the wound. (B courtesy of R. Aloni.)

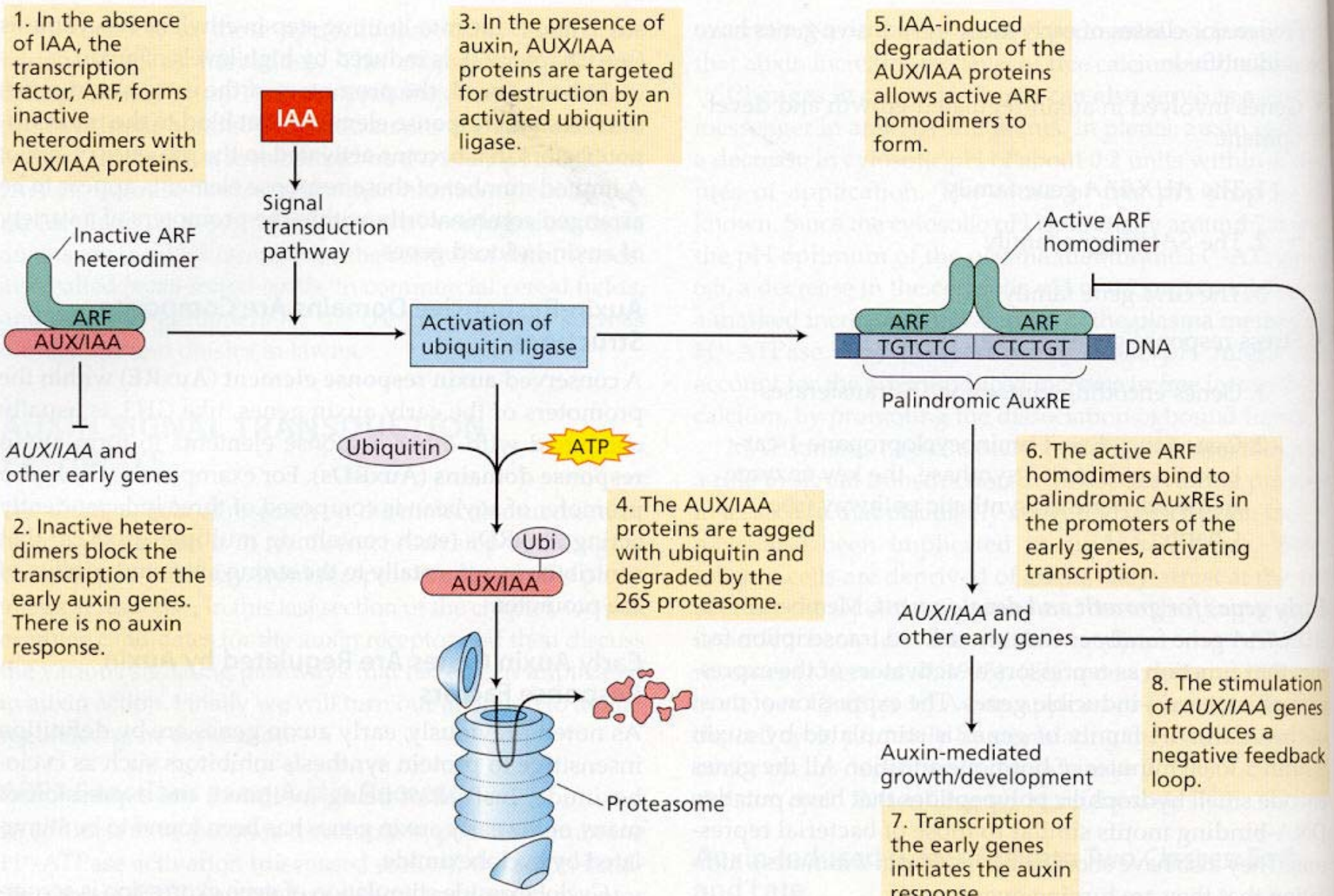

FIGURE 19.41 A model for auxin regulation of transcriptional activation of early response genes by auxin. (After Gray et al. 2001.)